

*Measurements of processes sensitive to quartic
electroweak couplings in ATLAS*

XII International Conference on New Frontiers in Physics, Crete, Greece

10th -23rd July 2023

Shalu Solomon

on behalf of the ATLAS Collaboration



Brandeis
UNIVERSITY



Introduction

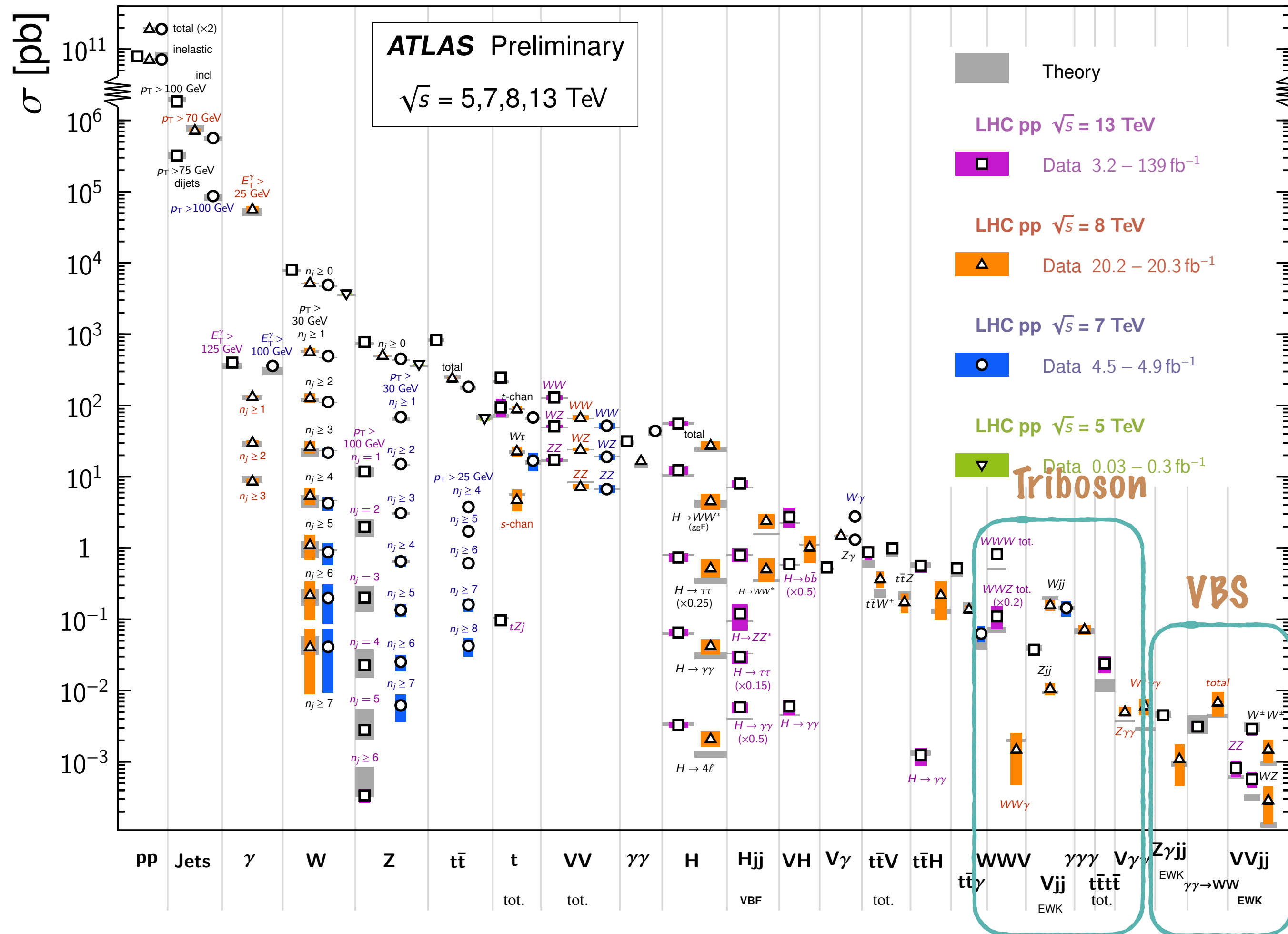
- Multiboson interactions serve as a stringent test of the Standard Model
- The non-Abelian nature of the electroweak theory allows for triple and quartic gauge interactions
- Diboson production via vector boson scattering (VBS) and triboson production are direct probes of tree-level quartic gauge couplings
- Test the Standard Model predictions for gauge boson self-interactions and electroweak symmetry breaking with the Higgs mechanism
- Study BSM effects by parametrizing any deviations from the Standard Model using the Effective Field Theory (EFT) such as anomalous triple/quartic gauge couplings

$$\mathcal{L}_{SMEFT} = \mathcal{L}_{SM} + \sum_i \frac{c_i^{d=6}}{\Lambda^2} \mathcal{O}^{d=6} + \sum_i \frac{c_i^{d=8}}{\Lambda^4} \mathcal{O}^{d=8} + \dots$$

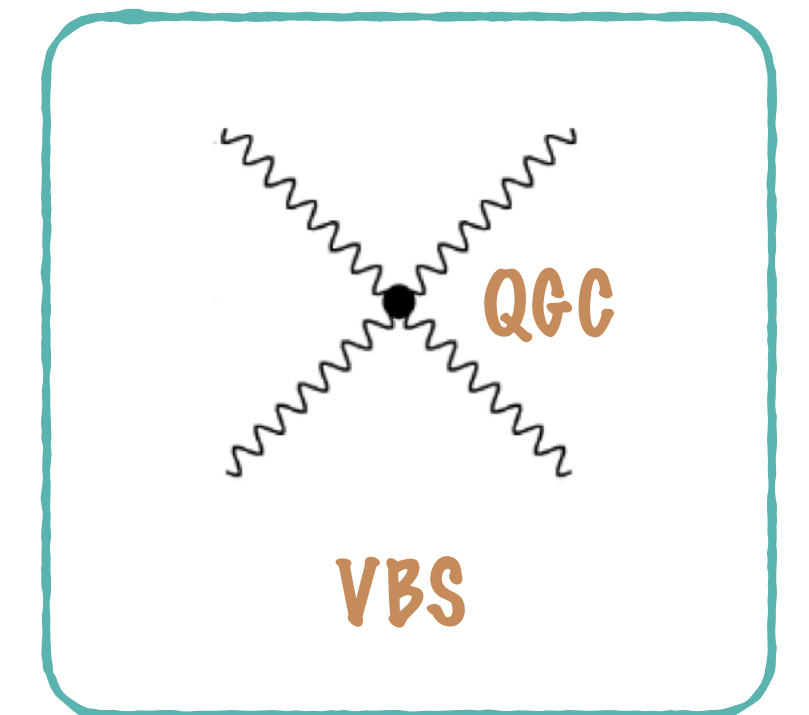
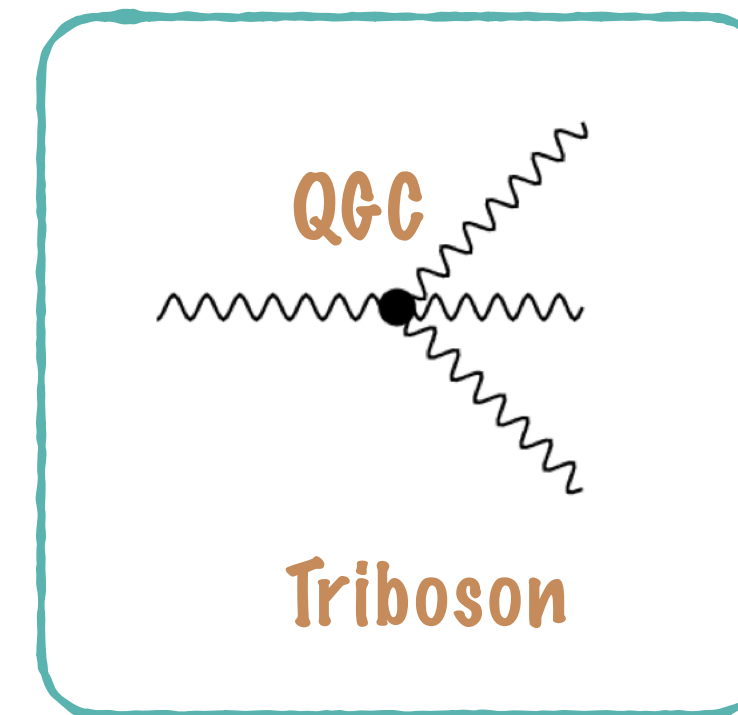
Introduction

Standard Model Production Cross Section Measurements

Status: February 2022



- Amongst the rarest processes studied at the LHC

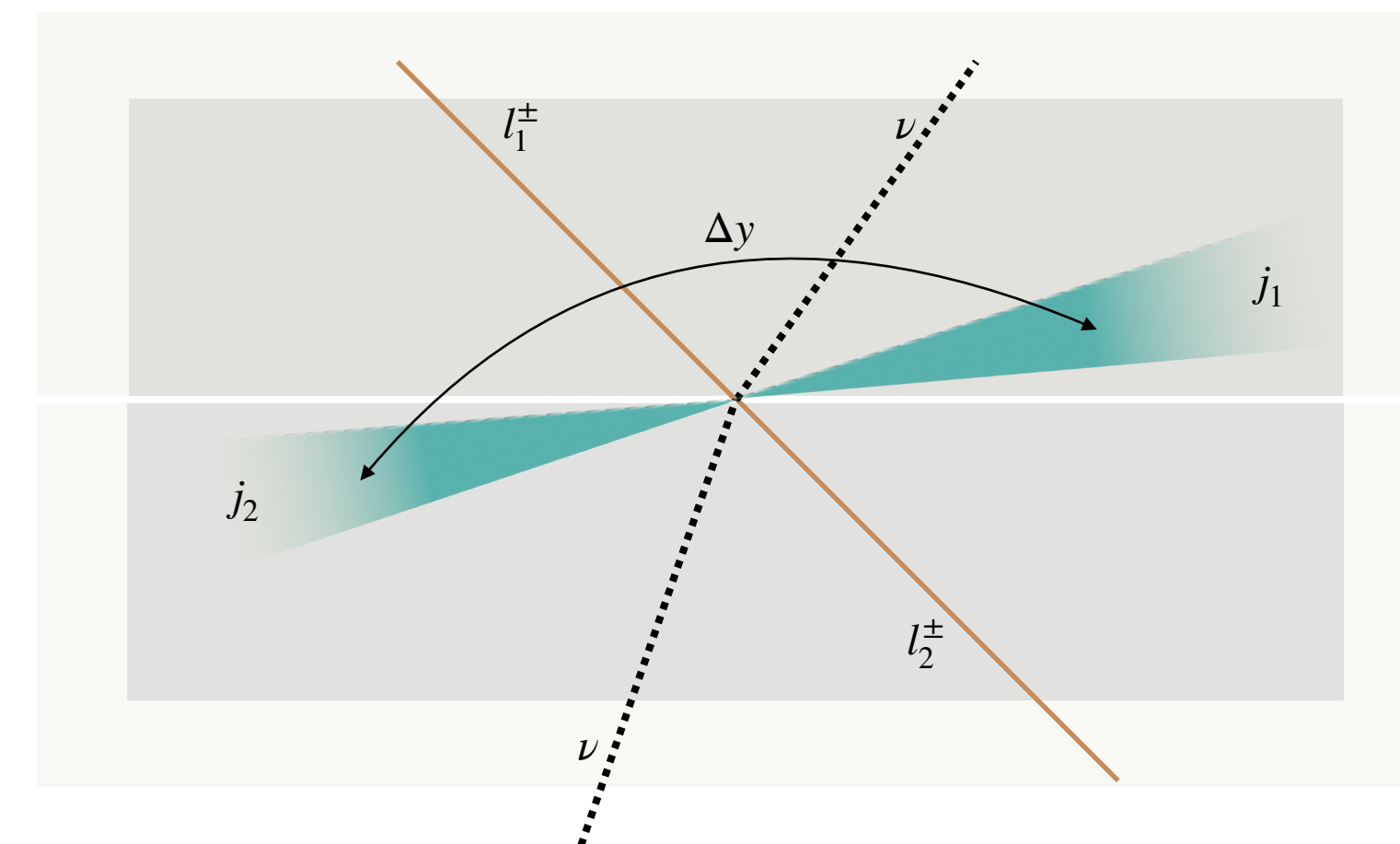
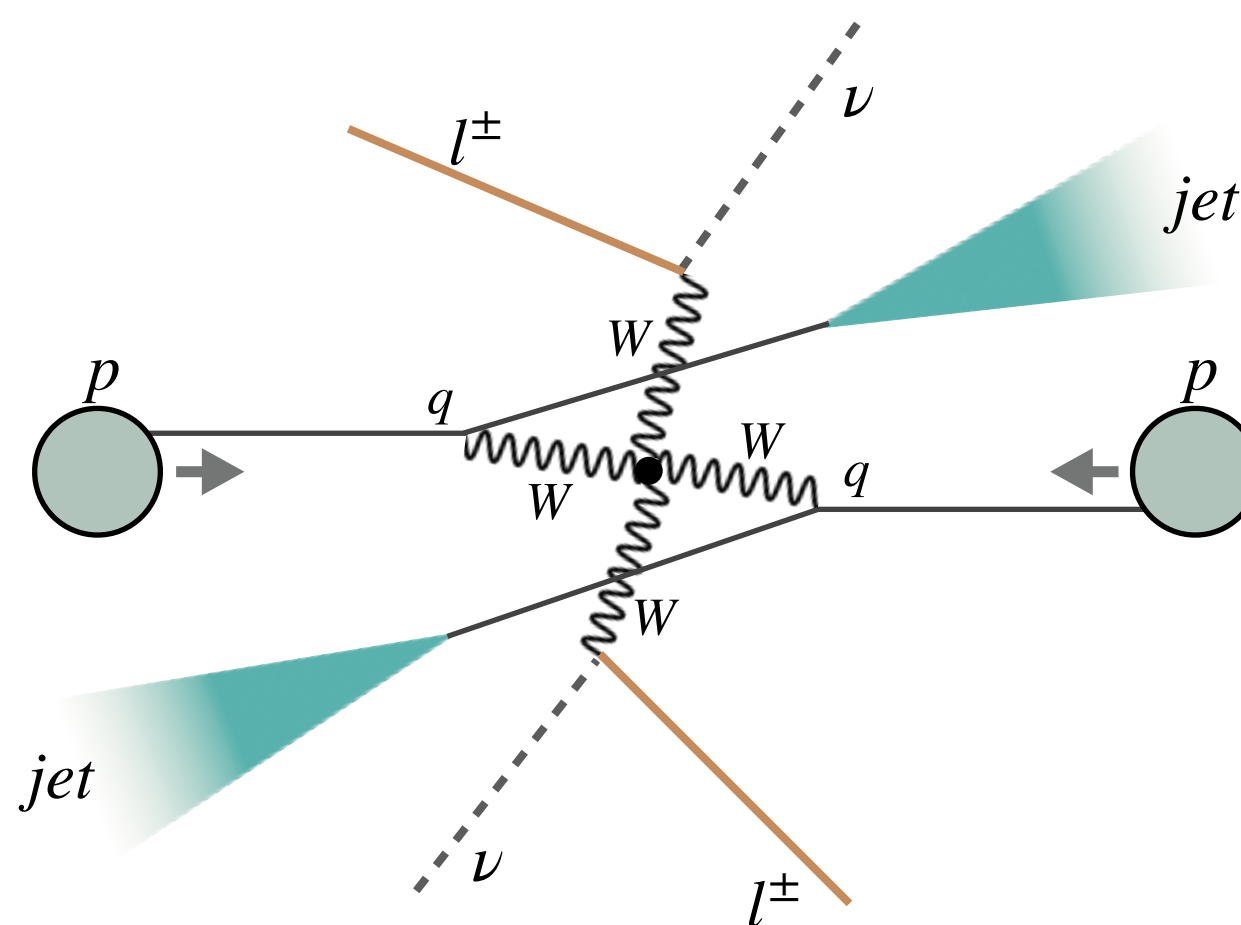


- In the Standard Model, the interactions involve a pair of W bosons

Overview

Vector boson scattering

- Two electroweak gauge bosons produced but with a distinct signature of two jets with a large dijet invariant mass m_{jj} and angular separation Δy_{jj}
- Little hadronic activity in the rapidity gap (centrality)



Triboson production

- Three electroweak gauge bosons produced in the hard scatter

Recent results in ATLAS covered today

Run 2 at $\sim 140 \text{ fb}^{-1}$

VBS: $W^\pm W^\pm jj$ $ZZjj$ $Z(ll)\gamma jj$ $Z(\nu\nu)\gamma jj$
Triboson: $Z\gamma\gamma$ $W\gamma\gamma$ $WZ\gamma$

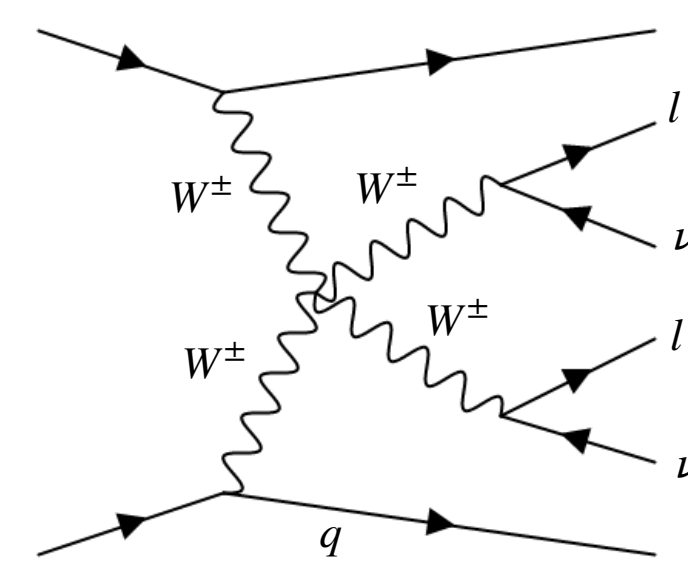
$W^\pm W^\pm (\rightarrow 2l2\nu) + \text{jets}$

Golden channel of VBS

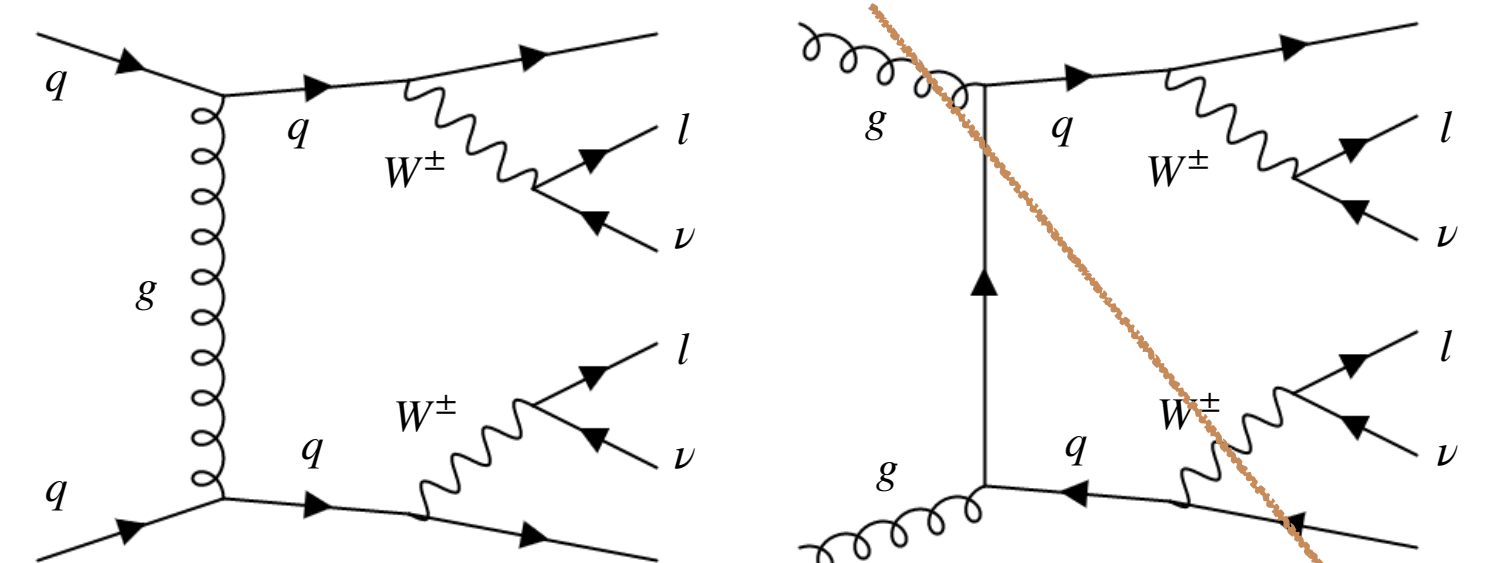
- No gg or qg initiating diagrams
- Largest electroweak to strong production ratio among other VV
- Final state with 2 same-sign leptons
- Small background rates due to the same-sign leptons in the final state

Cross-section measurement

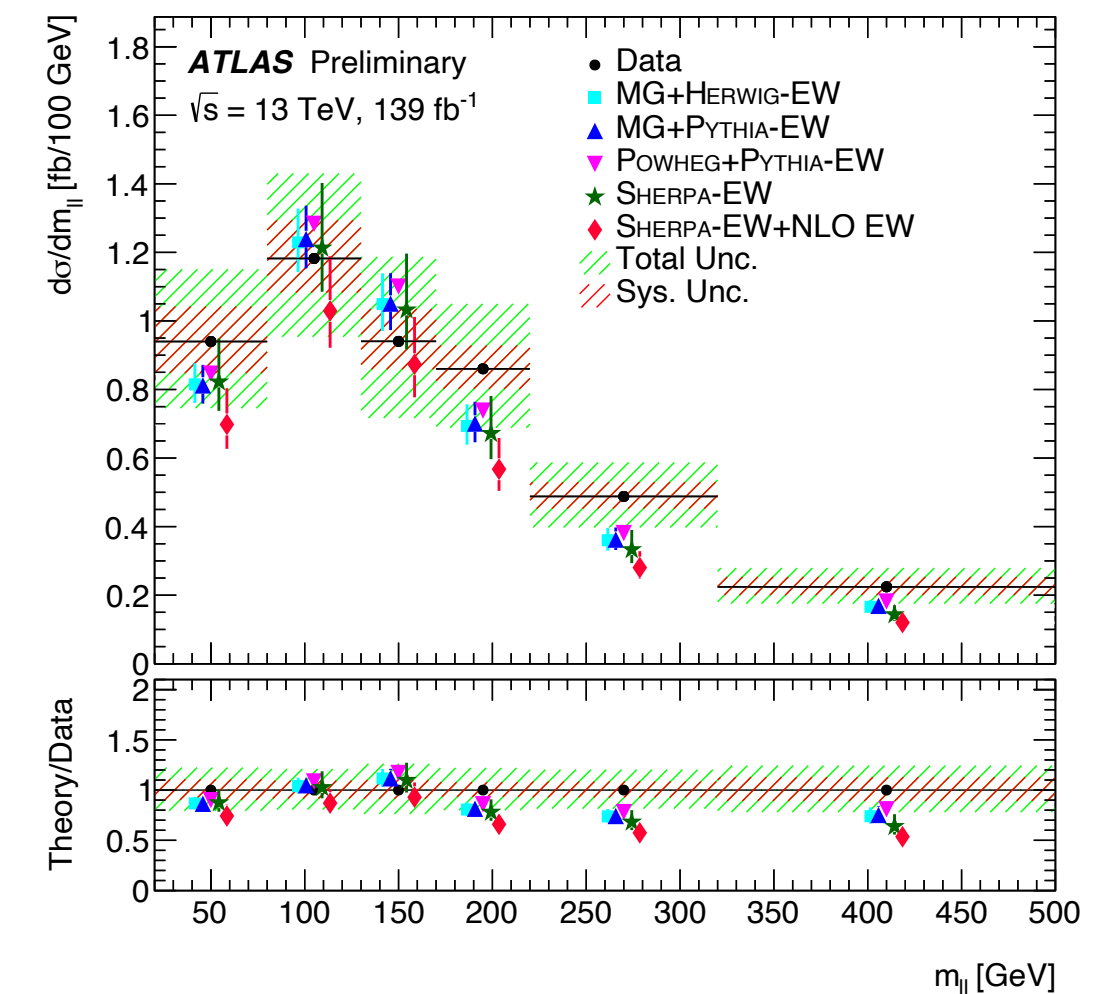
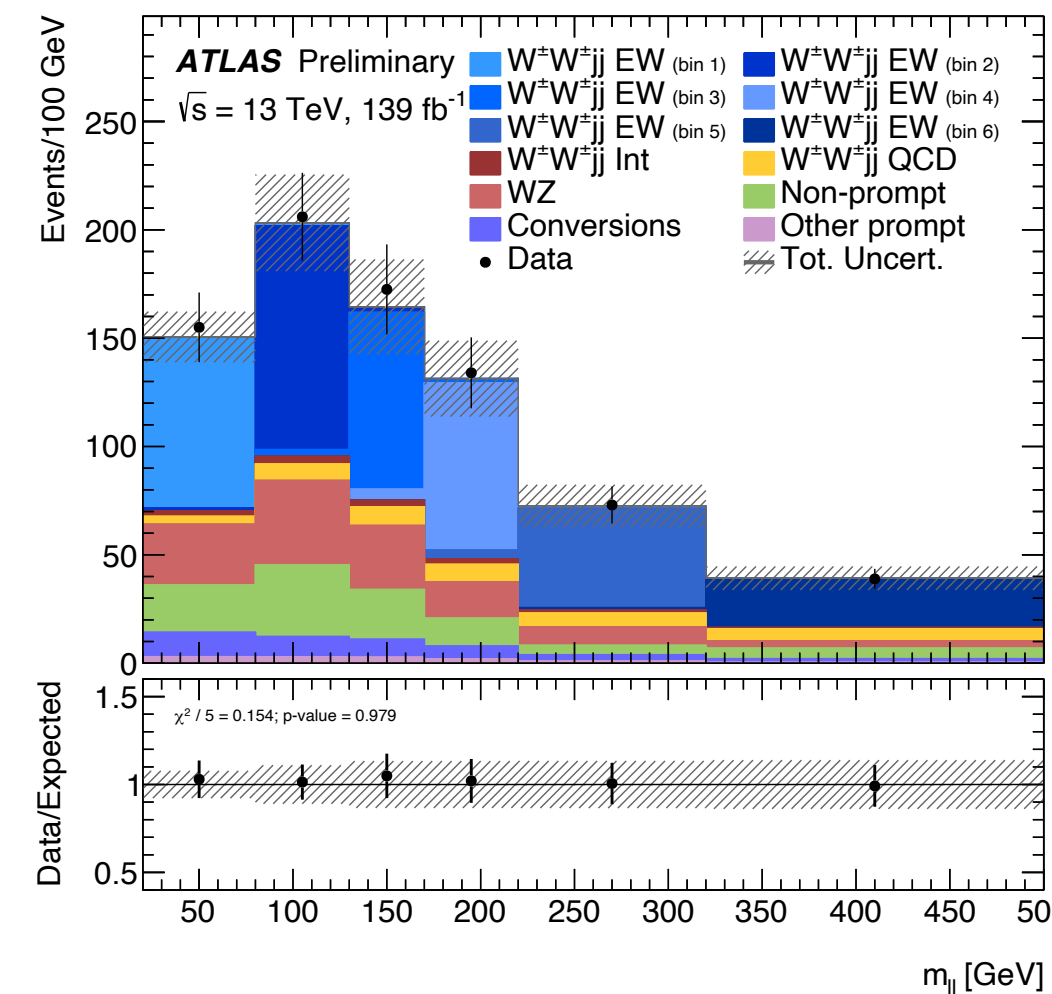
- Dominant backgrounds from WZ and mis-identified leptons
- Signal extracted from a simultaneous maximum likelihood 2D fit in SR and 3 lepton WZ-QCD CR



electroweak



strong



- Differential cross-section measured for electroweak (shown) and inclusive production (backup)
- Likelihood based unfolding for correction to particle level
- Leading uncertainty from data statistics

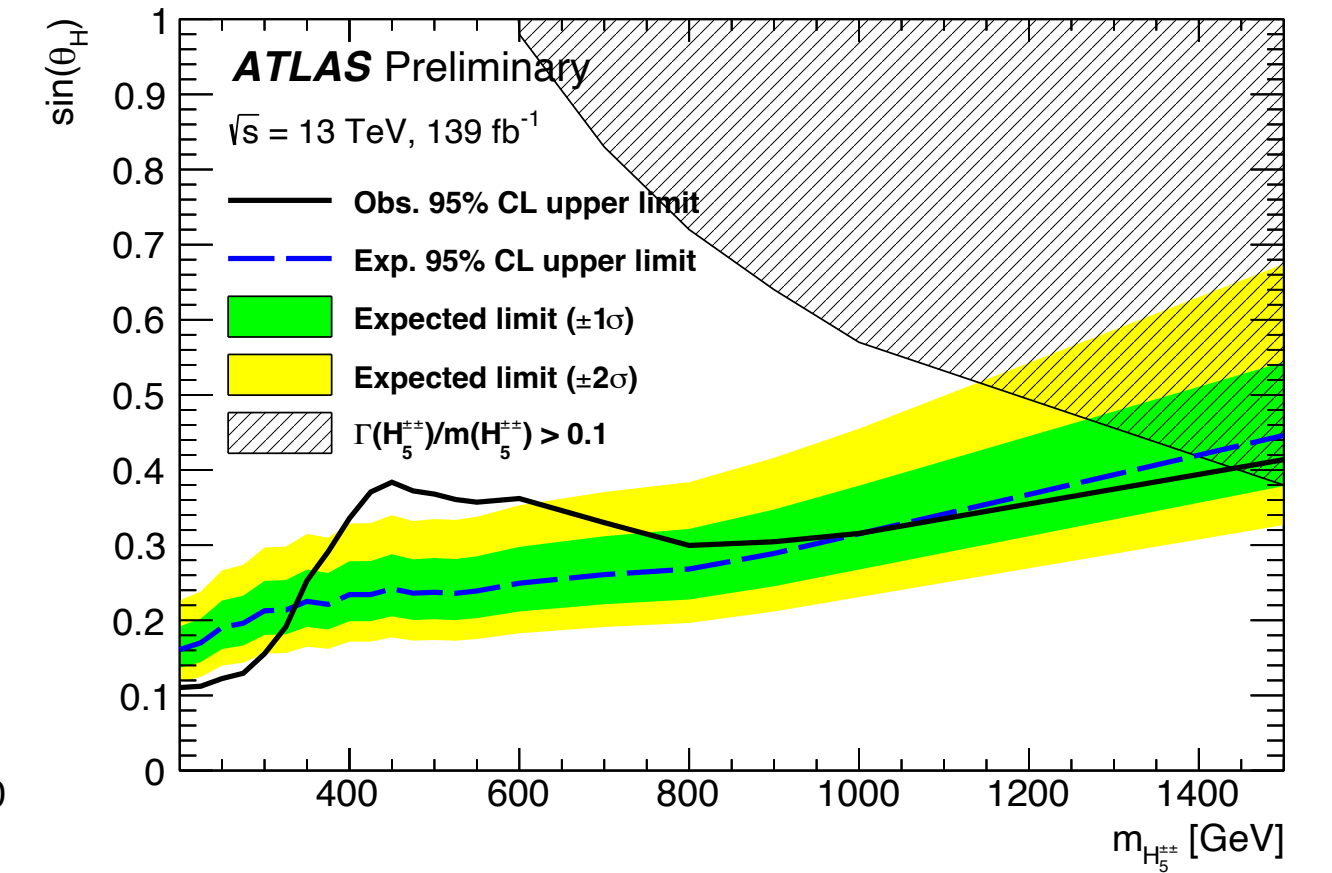
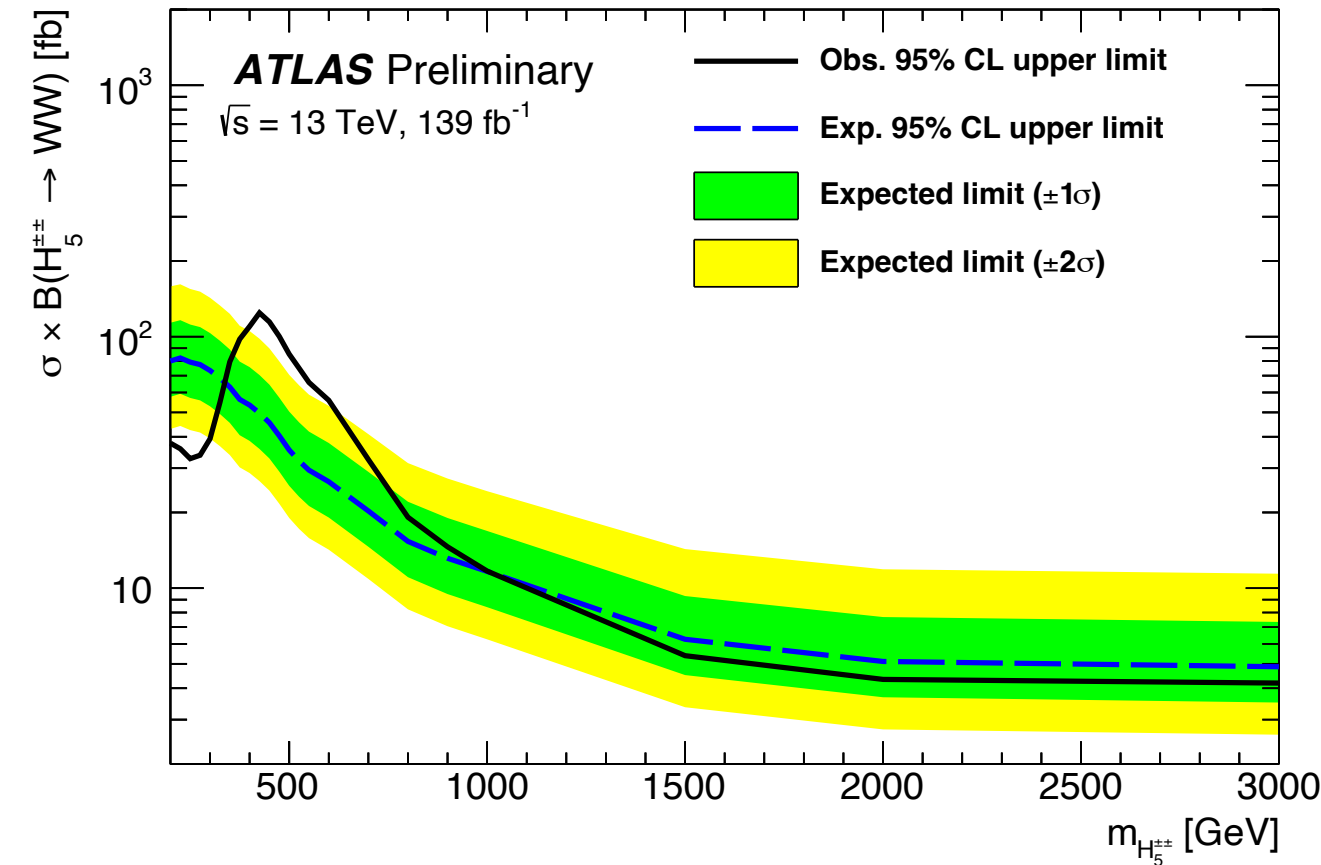
$W^\pm W^\pm$ SR
 $m_{jj} > 500$ GeV
 $\Delta y_{jj} > 2$

WZ-QCD CR
 $m_{jj} > 200$ GeV
 $\Delta y_{jj} > 2$

$W^\pm W^\pm (\rightarrow 2l/2\nu) + \text{jets}$

Search for doubly charged Higgs

- Results interpreted to search for $H^{\pm\pm}$ produced through vector boson fusion in the context of Georgi-Machacek model using $m_{H^{\pm\pm}}$ and $\sin\theta_H$ as model parameters
- Model independent upper limits at 95% CL on $\sigma(H^{\pm\pm}) \times B(H^{\pm\pm} \rightarrow W^\pm W^\pm)$ extracted
- Largest excess observed for $m_{H_5^{\pm\pm}} = 450 \text{ GeV}$ at 2.5σ
- $\sin\theta_H > 0.11-0.41$ are excluded for $200 < m_{H_5^{\pm\pm}} < 1500 \text{ GeV}$



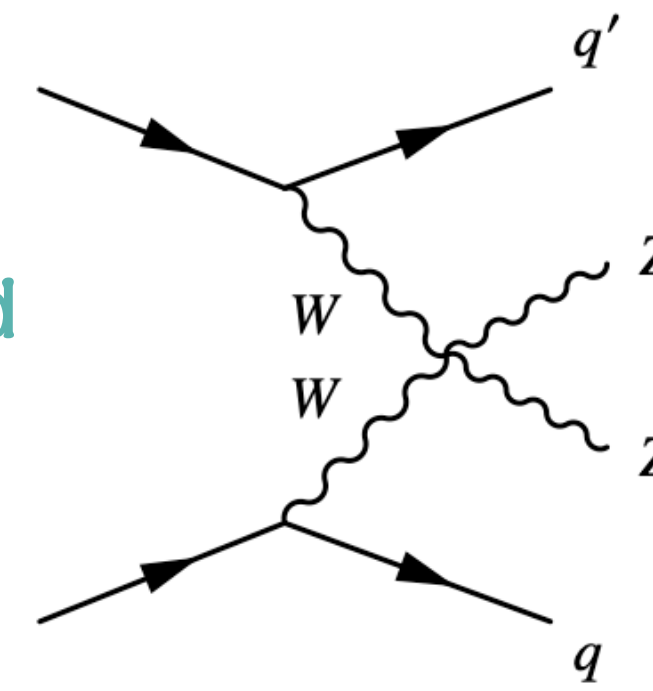
Search for aQGCs

- Results are interpreted within the EFT framework and limits are set on 8 Dim-8 operators
- Limits on a given Wilson coefficient are derived by setting all others to zero. Constraints are consistent with zero
- Limits are also obtained by removing EFT contributions above a certain energy scale E_c that violates unitarity (clipping) and restricting $m_{WW} < E_c$. E_c is evaluated using boson kinematics at parton level (before parton showering)

Coefficient	Type	No unitarisation cut-off [TeV ⁻⁴]	Lower and upper limit at the respective unitarity bound [TeV ⁻⁴]
f_{M0}/Λ^4	exp.	[-3.9, 3.8]	-64 at 0.9 TeV, 40 at 1.0 TeV
	obs.	[-4.1, 4.1]	-140 at 0.7 TeV, 117 at 0.8 TeV
f_{M1}/Λ^4	exp.	[-6.3, 6.6]	-25.5 at 1.6 TeV, 31 at 1.5 TeV
	obs.	[-6.8, 7.0]	-45 at 1.4 TeV, 54 at 1.3 TeV
f_{M7}/Λ^4	exp.	[-9.3, 8.8]	-33 at 1.8 TeV, 29.1 at 1.8 TeV
	obs.	[-9.8, 9.5]	-39 at 1.7 TeV, 42 at 1.7 TeV
f_{S02}/Λ^4	exp.	[-5.5, 5.7]	-94 at 0.8 TeV, 122 at 0.7 TeV
	obs.	[-5.9, 5.9]	—
f_{S1}/Λ^4	exp.	[-22.0, 22.5]	—
	obs.	[-23.5, 23.6]	—
f_{T0}/Λ^4	exp.	[-0.34, 0.34]	-3.2 at 1.2 TeV, 4.9 at 1.1 TeV
	obs.	[-0.36, 0.36]	-7.4 at 1.0 TeV, 12.4 at 0.9 TeV
f_{T1}/Λ^4	exp.	[-0.158, 0.174]	-0.32 at 2.6 TeV, 0.44 at 2.4 TeV
	obs.	[-0.174, 0.186]	-0.38 at 2.5 TeV, 0.49 at 2.4 TeV
f_{T2}/Λ^4	exp.	[-0.56, 0.70]	-2.60 at 1.7 TeV, 10.3 at 1.2 TeV
	obs.	[-0.63, 0.74]	—

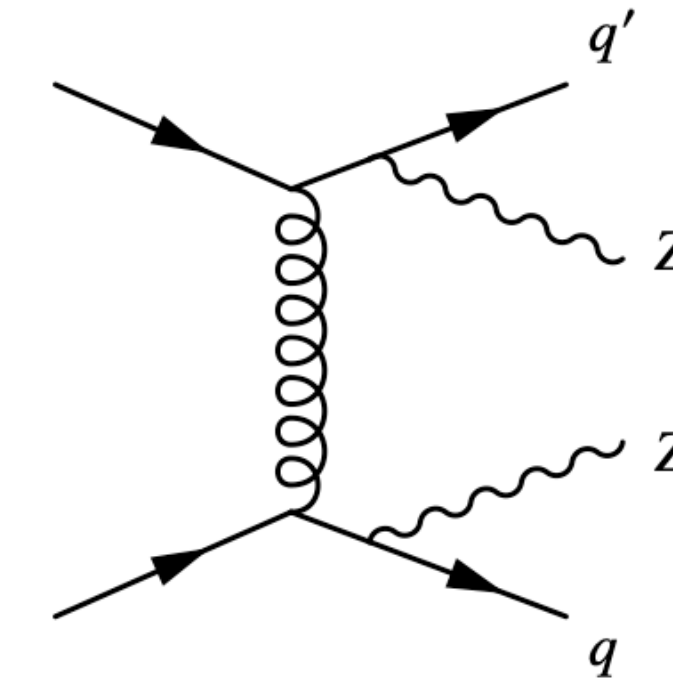
ZZ($\rightarrow 4l$) + jets

sensitive to WWZ and WWZZ interactions



electroweak

sensitive to perturbative QCD calculations



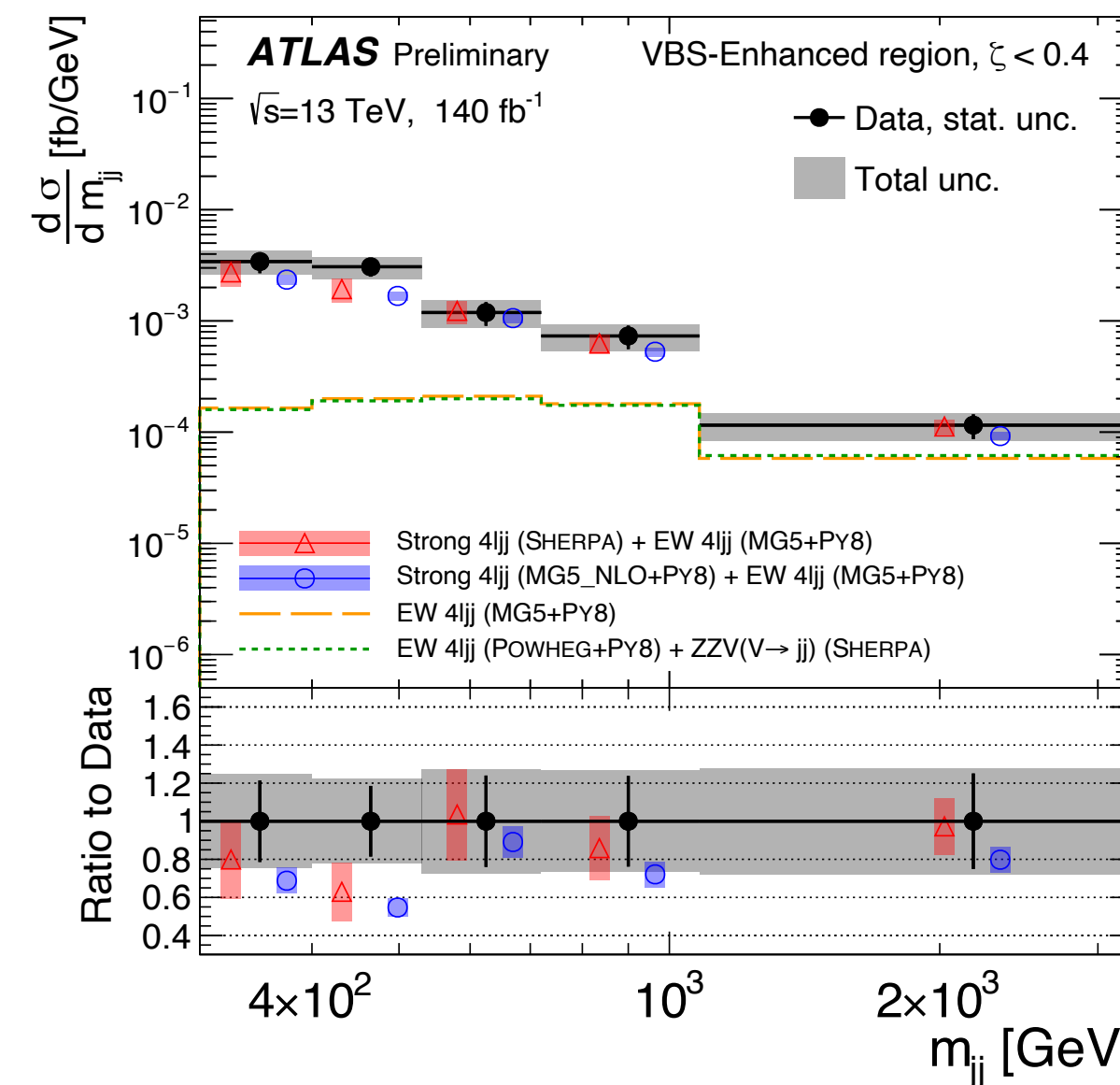
strong

- Two l^+l^- pairs with the smallest $|m_{ll} - m_Z|$
- $m_{4l} > 130$ GeV
- Differential cross-section measurement for inclusive production in two SRs based on $4l$ centrality

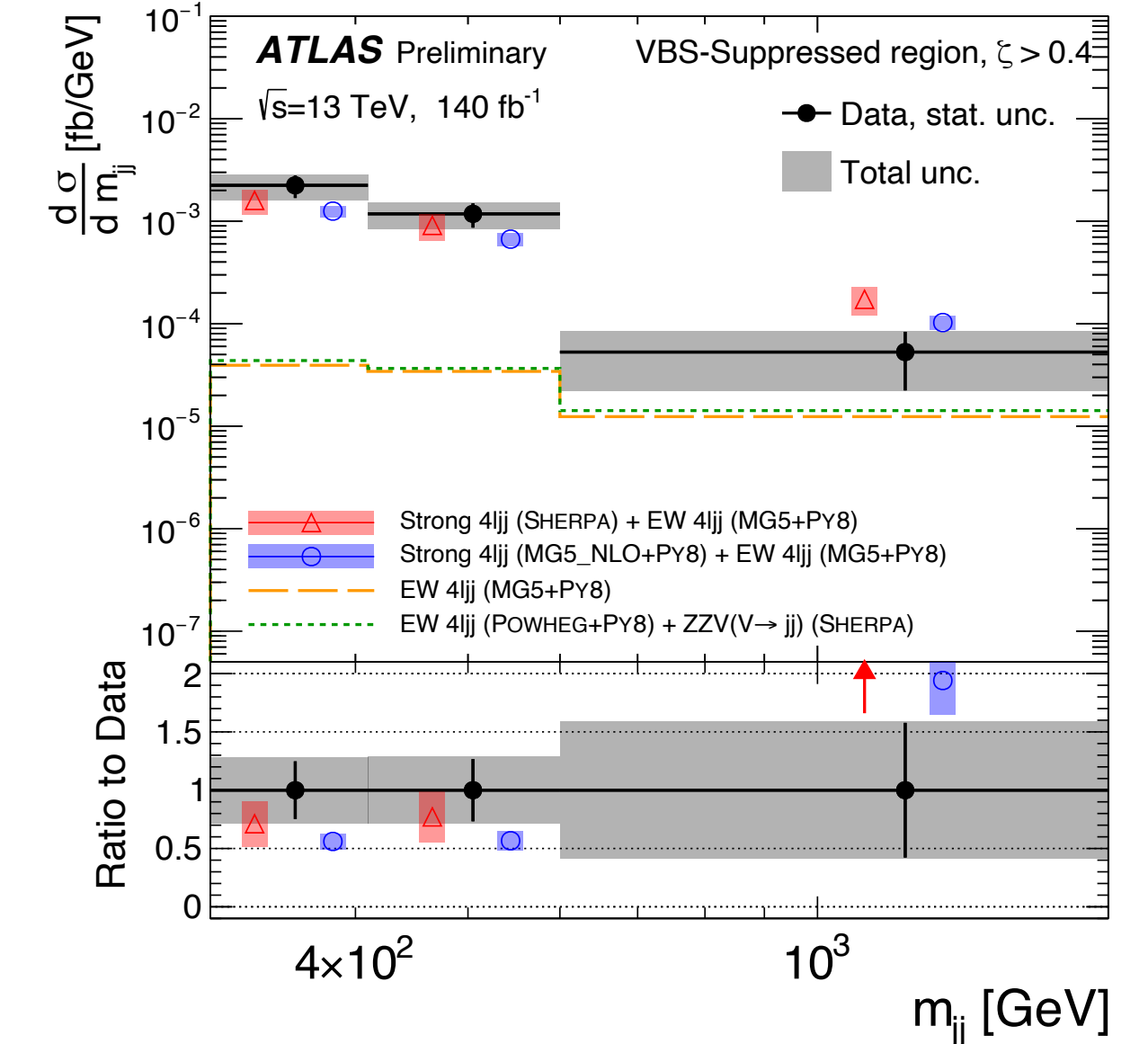
- VBS enhanced SR with $\zeta < 0.4$
- VBS suppressed SR with $\zeta > 0.4$

$$\zeta = \frac{y_{4l} - 0.5(y_{j_1} + y_{j_2})}{\Delta y_{jj}}$$

- Measurements sensitive to ZZ-QCD signal modelling
 - MadGraph predictions for strong production underestimate the cross-section in both SRs
 - Mis-modelling in Sherpa at high m_{jj} in VBS suppressed SR



VBS enhanced



VBS suppressed

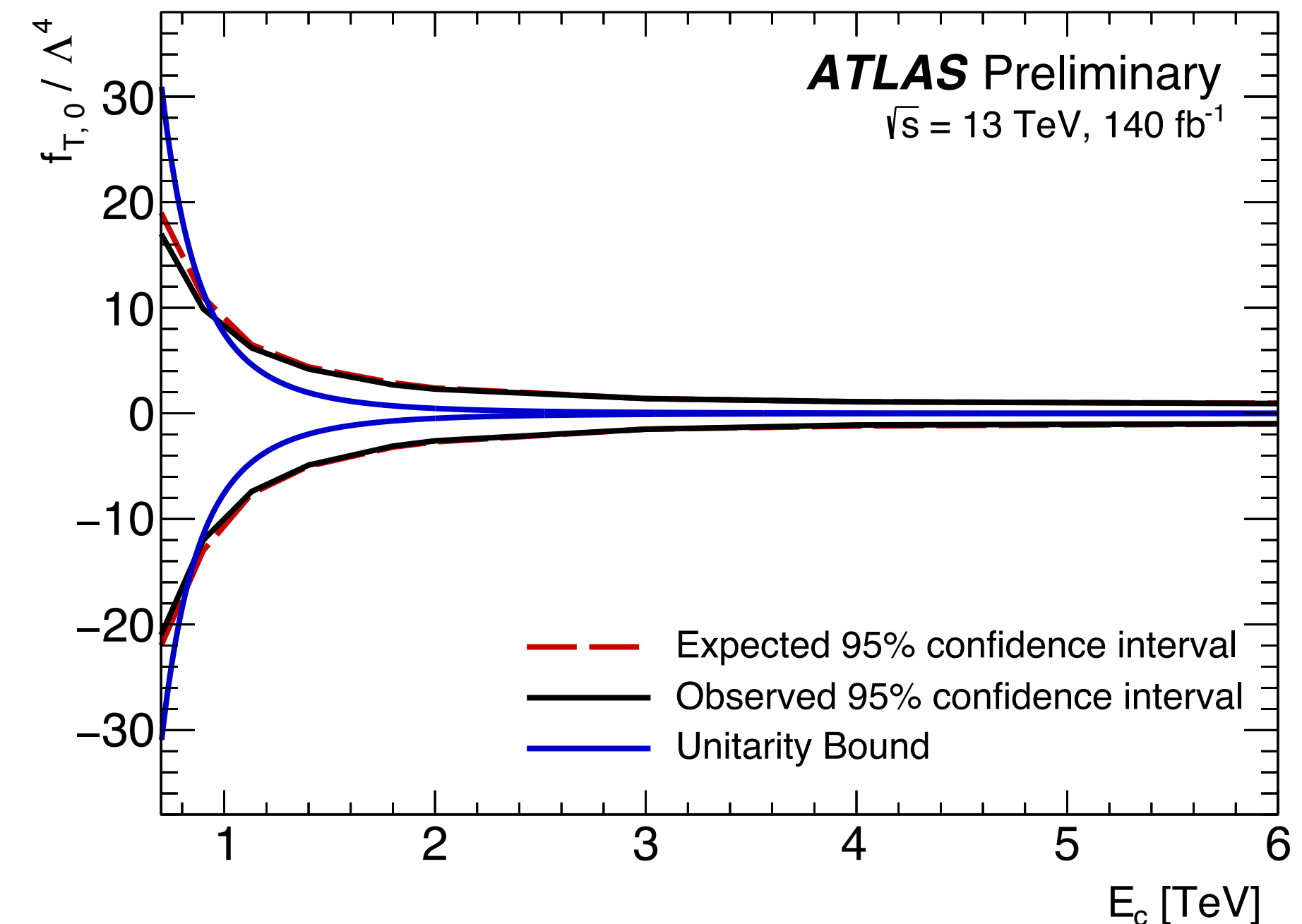
ZZ($\rightarrow 4l$) + jets

- A 2D fit of the differential cross-section as a function of m_{4l} and m_{jj} are used to set limits on Dim-6 and Dim-8 EFT operators

Wilson coefficient	$ \mathcal{M}_{d8} ^2$ Included	95% confidence interval [TeV^{-4}]	
		Expected	Observed
$f_{T,0}/\Lambda^4$	yes	[-0.98, 0.93]	[-1.0, 0.97]
	no	[-23, 17]	[-19, 19]
$f_{T,1}/\Lambda^4$	yes	[-1.2, 1.2]	[-1.3, 1.3]
	no	[-160, 120]	[-140, 140]
$f_{T,2}/\Lambda^4$	yes	[-2.5, 2.4]	[-2.6, 2.5]
	no	[-74, 56]	[-63, 62]
$f_{T,5}/\Lambda^4$	yes	[-2.5, 2.4]	[-2.6, 2.5]
	no	[-79, 60]	[-68, 67]
$f_{T,6}/\Lambda^4$	yes	[-3.9, 3.9]	[-4.1, 4.1]
	no	[-64, 48]	[-55, 54]
$f_{T,7}/\Lambda^4$	yes	[-8.5, 8.1]	[-8.8, 8.4]
	no	[-260, 200]	[-220, 220]
$f_{T,8}/\Lambda^4$	yes	[-2.1, 2.1]	[-2.2, 2.2]
	no	$[-4.6, 3.1] \times 10^4$	$[-3.9, 3.8] \times 10^4$
$f_{T,9}/\Lambda^4$	yes	[-4.5, 4.5]	[-4.7, 4.7]
	no	$[-7.5, 5.5] \times 10^4$	$[-6.4, 6.3] \times 10^4$

- Results are shown when pure Dim-8 contribution is included and excluded in the theoretical predictions
- Wilson coefficients are consistent with zero

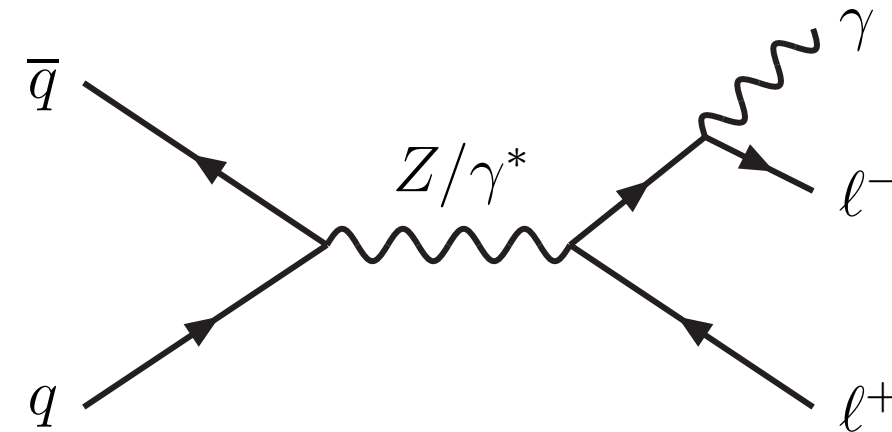
- Constraints are also placed after clipping: restricting the interference and pure Dim-8 contributions to have $m_{4l} < E_c$
- 95% CL intervals degrade by a factor of 4-5 when the energy scale cut off is reduced from $E_c = \infty$ to $E_c = 1 \text{ TeV}$



$Z\gamma(\rightarrow 2l\gamma) + \text{jets}$

First observation in ATLAS

- Probes neutral quartic gauge couplings but has a larger cross-section than ZZ
- Dominant background from $Z\gamma$ -QCD and non-prompt photons (jets misidentified as photons) from Z +jets
- FSR suppressed with $m_{ll} + m_{ll\gamma} > 182$ GeV



- Differential cross-section extracted from a maximum likelihood fit in SR and CR

$Z\gamma$ -EWK SR

$$m_{jj} > 500 \text{ GeV}$$

$$\zeta < 0.4$$

Inclusive $Z\gamma$ SR

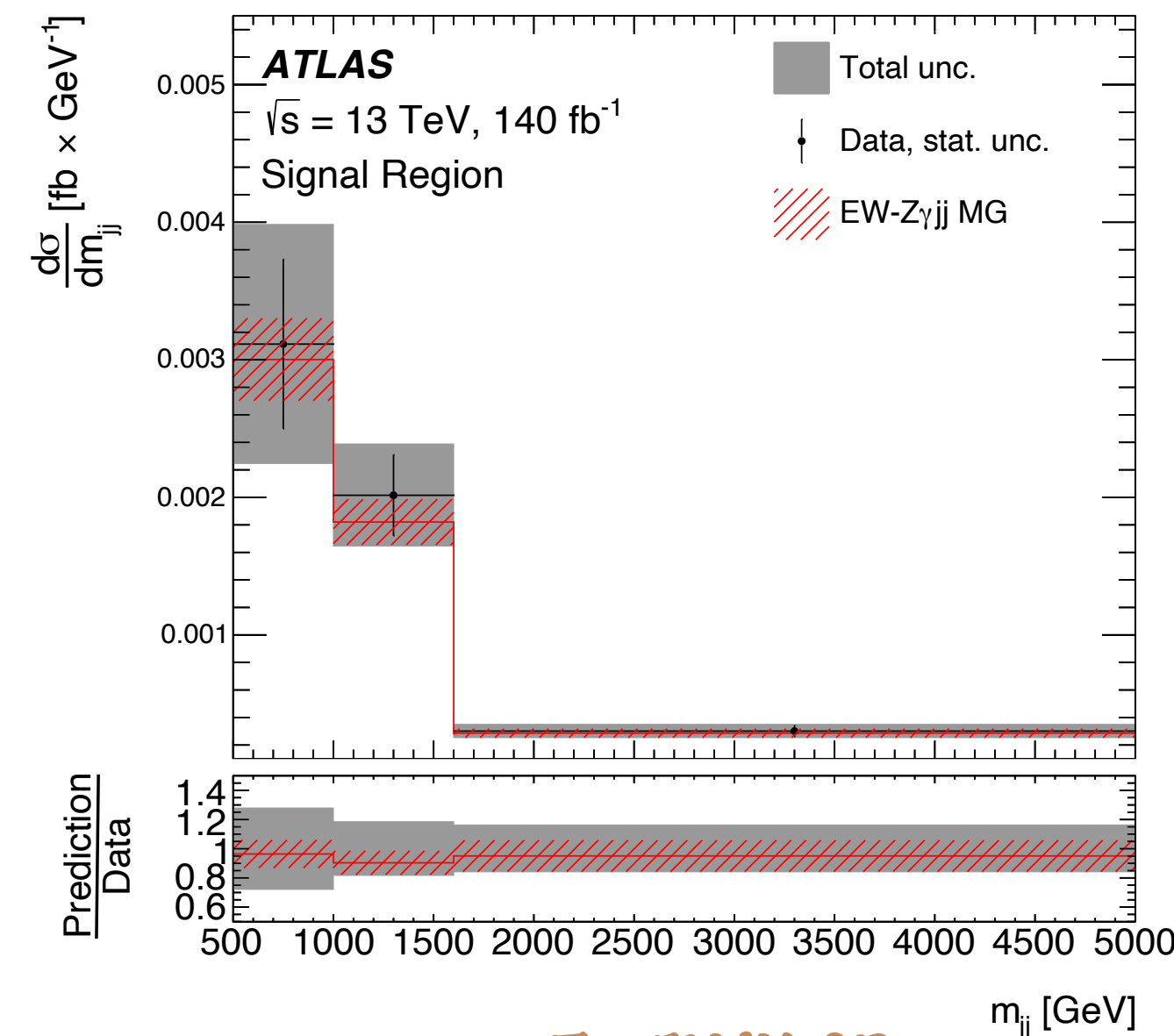
$$m_{jj} > 150 \text{ GeV}$$

$$\zeta < 0.4$$

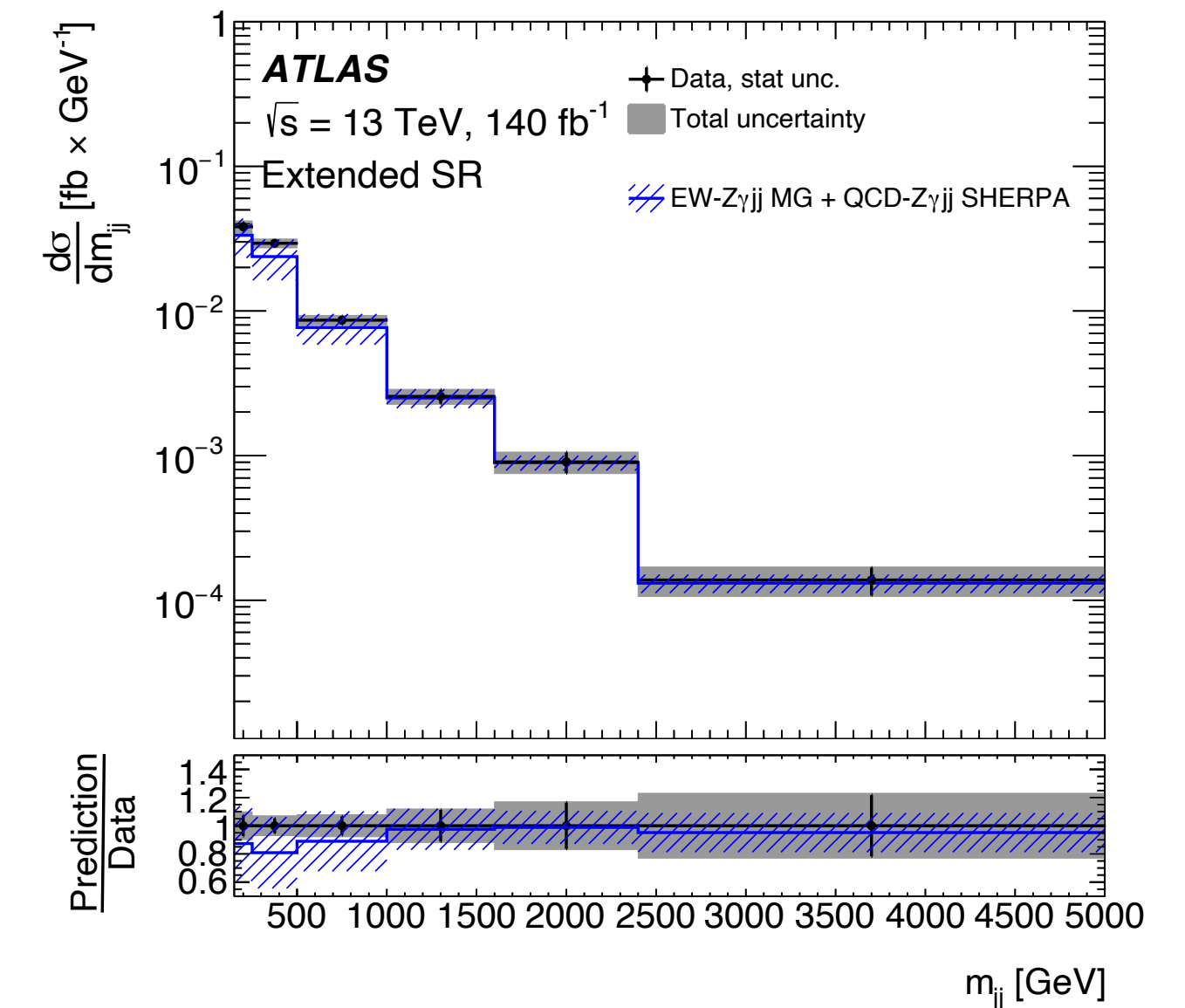
$Z\gamma$ -QCD CR

$$m_{jj} > 500 \text{ GeV}$$

$$\zeta > 0.4$$



$Z\gamma$ -EWK SR



Inclusive $Z\gamma$ SR

σ	Observed	Expected
$Z\gamma$ -EWK	3.6 ± 0.5 fb	3.5 ± 0.3 fb
$Z\gamma$	$16.8^{+2.0}_{-1.8}$ fb	$15.7^{+5.0}_{-2.6}$ fb

	Data stat.	MC stat.	Background	Reco	EW mod.	QCD mod.	Total
$\Delta\sigma_{EW}/\sigma_{EW}$ [%]	± 9	± 1	± 1	± 4	$+8$ -6	± 2	± 13
$\Delta\sigma_{Z\gamma}/\sigma_{Z\gamma}$ [%]	± 3	± 1	± 2	$+4$ -3	$+7$ -6	± 9	$+12$ -11

$Z\gamma(\rightarrow 2\nu\gamma) + \text{jets}$

First observation at the LHC

- Probes neutral quartic gauge couplings but larger BR for $Z \rightarrow \nu\bar{\nu}$ than $Z \rightarrow l^+l^-$
- Final state with an energetic photon $E_T^\gamma > 150$ GeV and large $E_T^{\text{miss}} > 120$ GeV
- Dominant backgrounds from $W\gamma$ and $Z\gamma$ -QCD
- Signal extracted from a binned maximum likelihood fit using a BDT classifier response in the SR and m_{jj} in $Z\gamma$ -QCD and $W\gamma$ CRs

$Z\gamma$ SR

$m_{jj} > 300$ GeV
 γ -centrality < 0.6

$Z\gamma$ -QCD CR1

$m_{jj} < 300$ GeV
 γ -centrality < 0.6

$Z\gamma$ -QCD CR2

$m_{jj} > 300$ GeV
 γ -centrality > 0.6

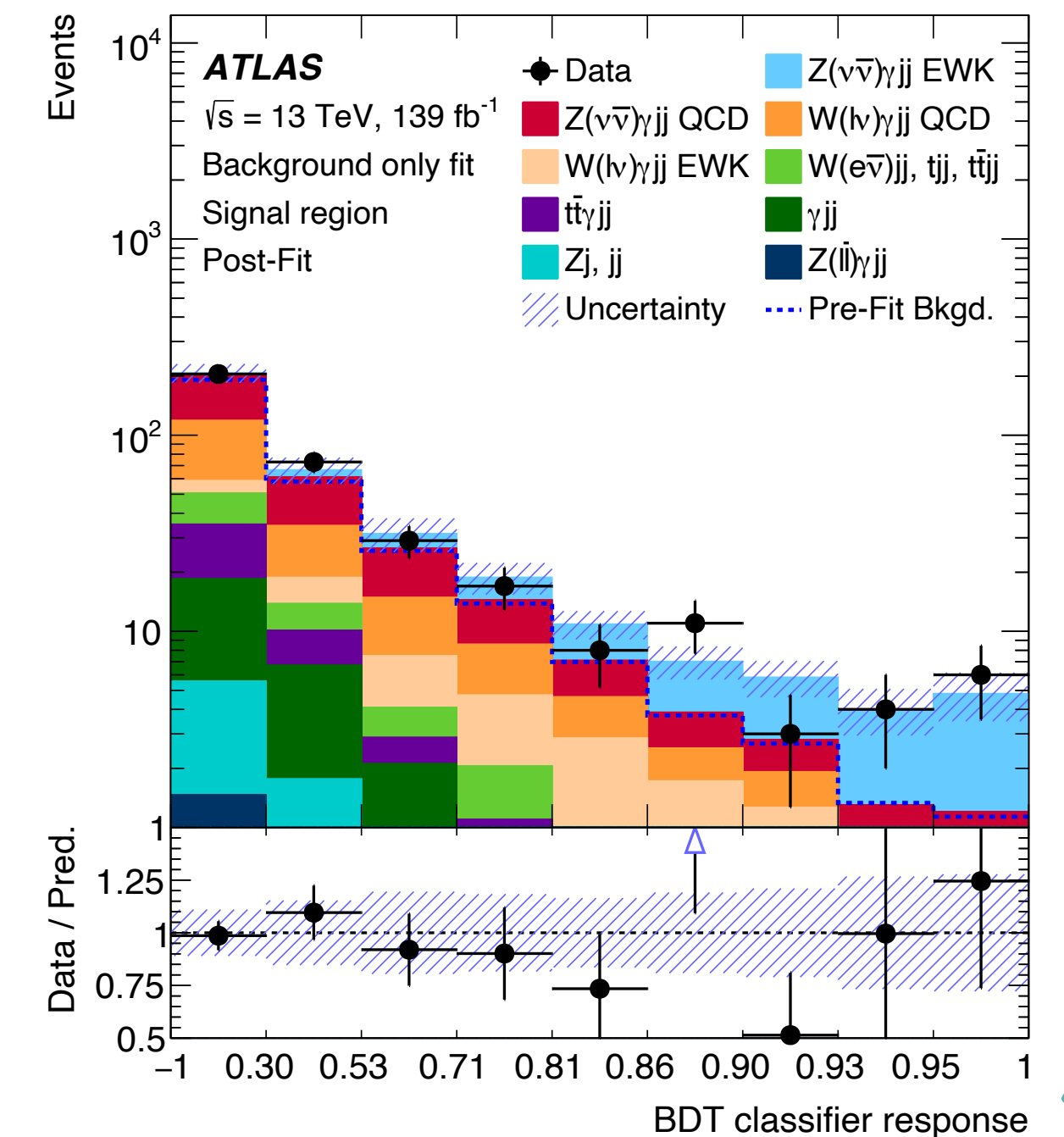
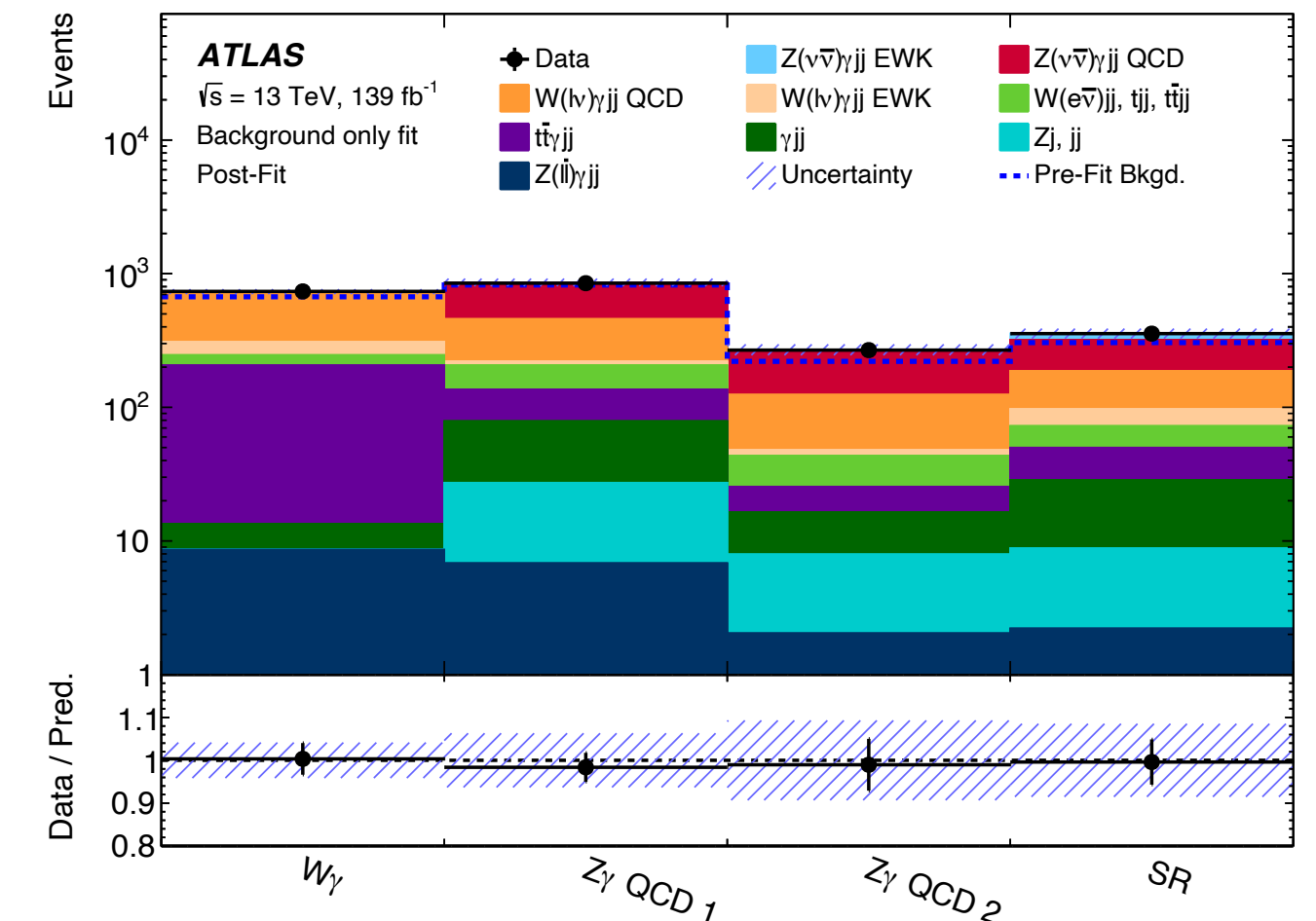
$W\gamma$ -QCD CR

$m_{jj} > 300$ GeV
 γ -centrality > 0.6
 1 lepton unlike SR

- Measured cross-section in agreement with SM predictions

$$\sigma_{fid} = 0.77^{+0.34}_{-0.30} \text{ fb}$$

Observed with 3.2σ (3.7σ expected)



$Z\gamma(\rightarrow 2\nu\gamma) + \text{jets}$

- Combination with a previous ATLAS measurement: **Observed with 6.3σ**

Eur. Phys. J. C 82 (2022) 105

$15 < E_T^\gamma < 110 \text{ GeV}$

Not sensitive to aQGC search

Observed with 5.2σ

started as a search for BSM Higgs decays

This analysis

$E_T^\gamma > 150 \text{ GeV}$

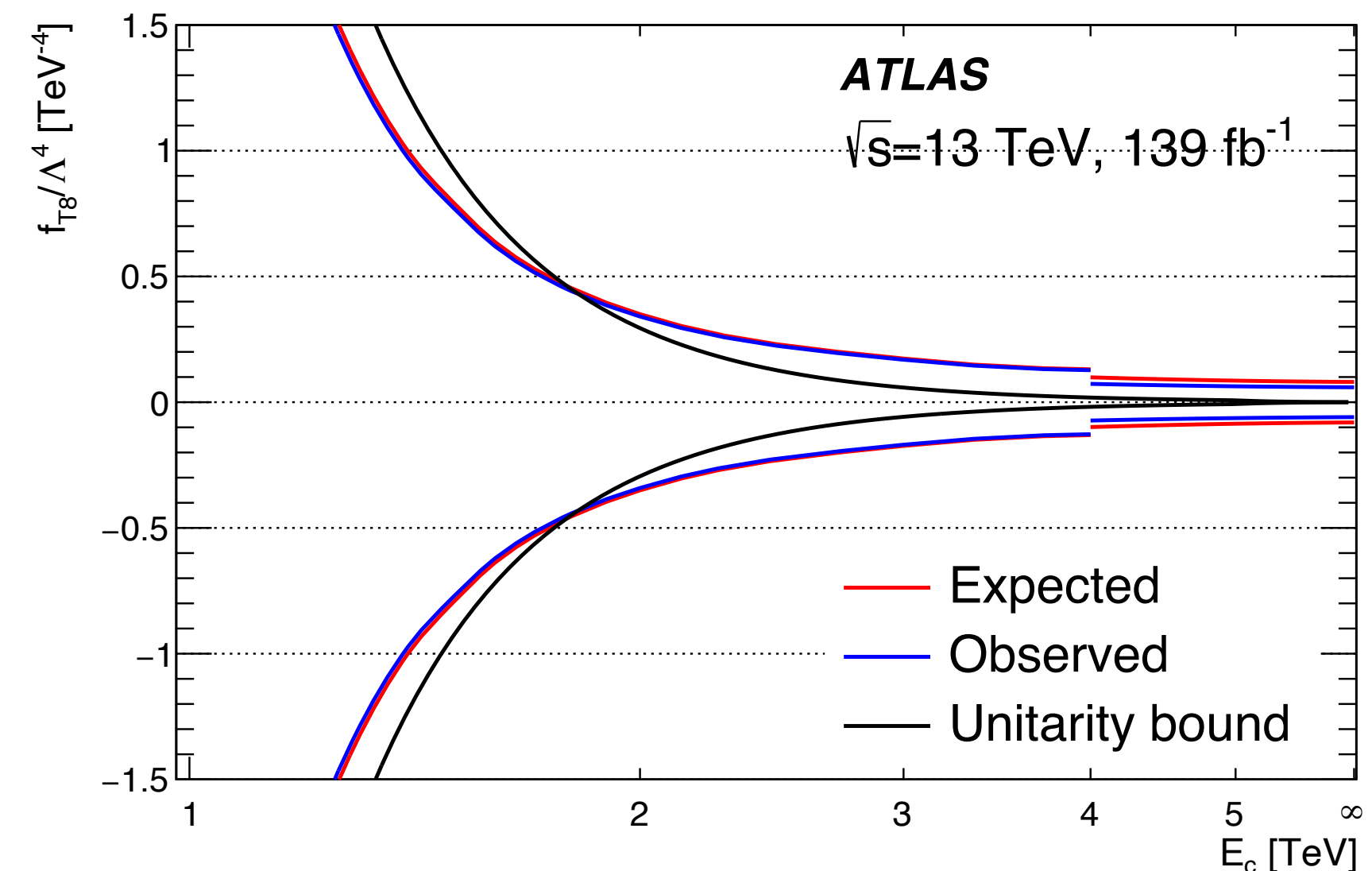
Sensitive to aQGC search

Observed with 3.2σ

POI	$15 < E_T^\gamma < 110 \text{ GeV}$	$E_T^\gamma > 150 \text{ GeV}$	Combination
$\mu_{Z\gamma\text{EWK}}$	0.78 ± 0.33	1.04 ± 0.23	0.96 ± 0.18
$\mu_{Z\gamma\text{QCD}}$	1.21 ± 0.37	1.02 ± 0.41	1.17 ± 0.27
$\mu_{W\gamma}$	1.02 ± 0.22	1.01 ± 0.20	1.01 ± 0.13

Combination increases the overall sensitivity to electroweak $Z\gamma$ +jets

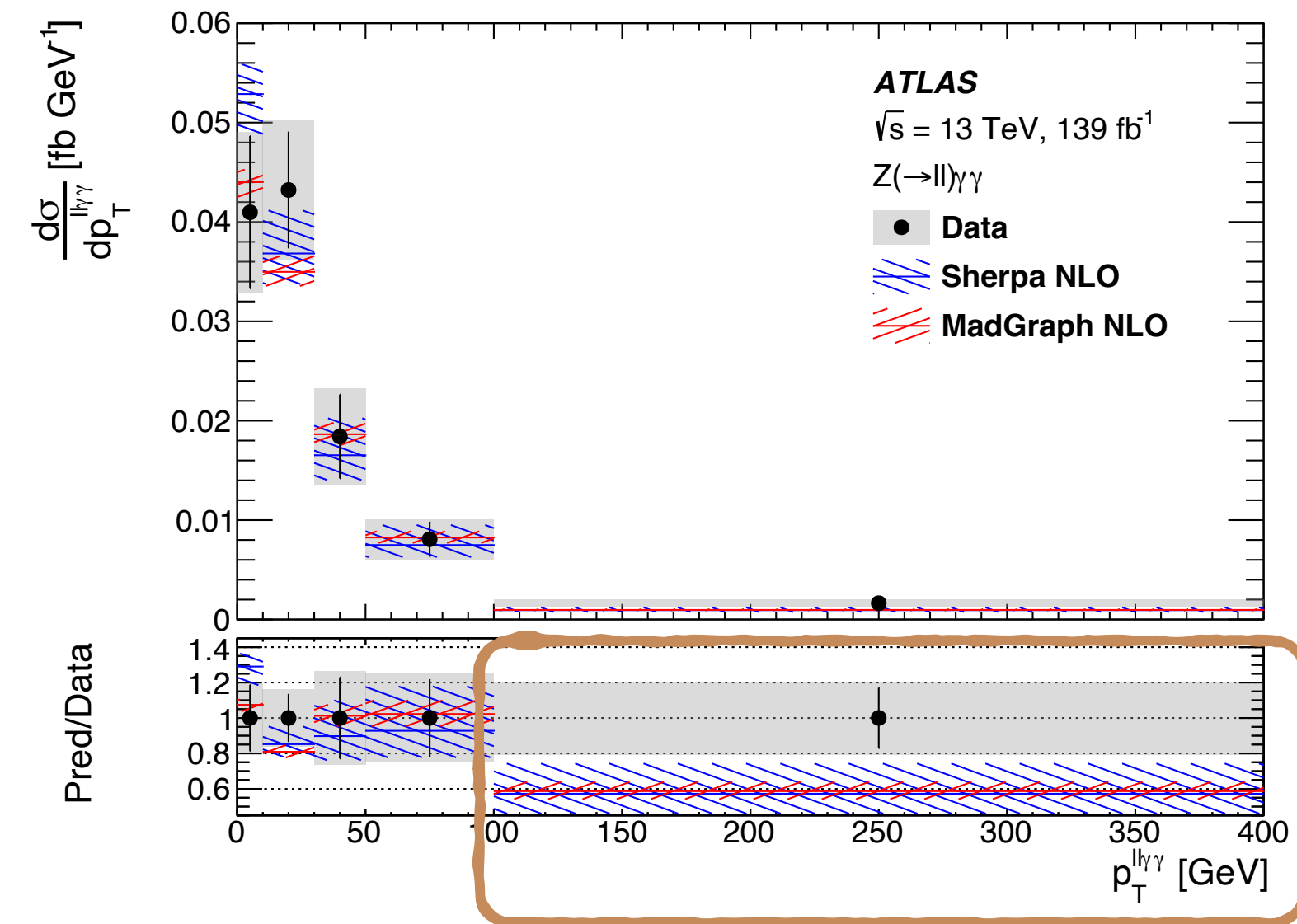
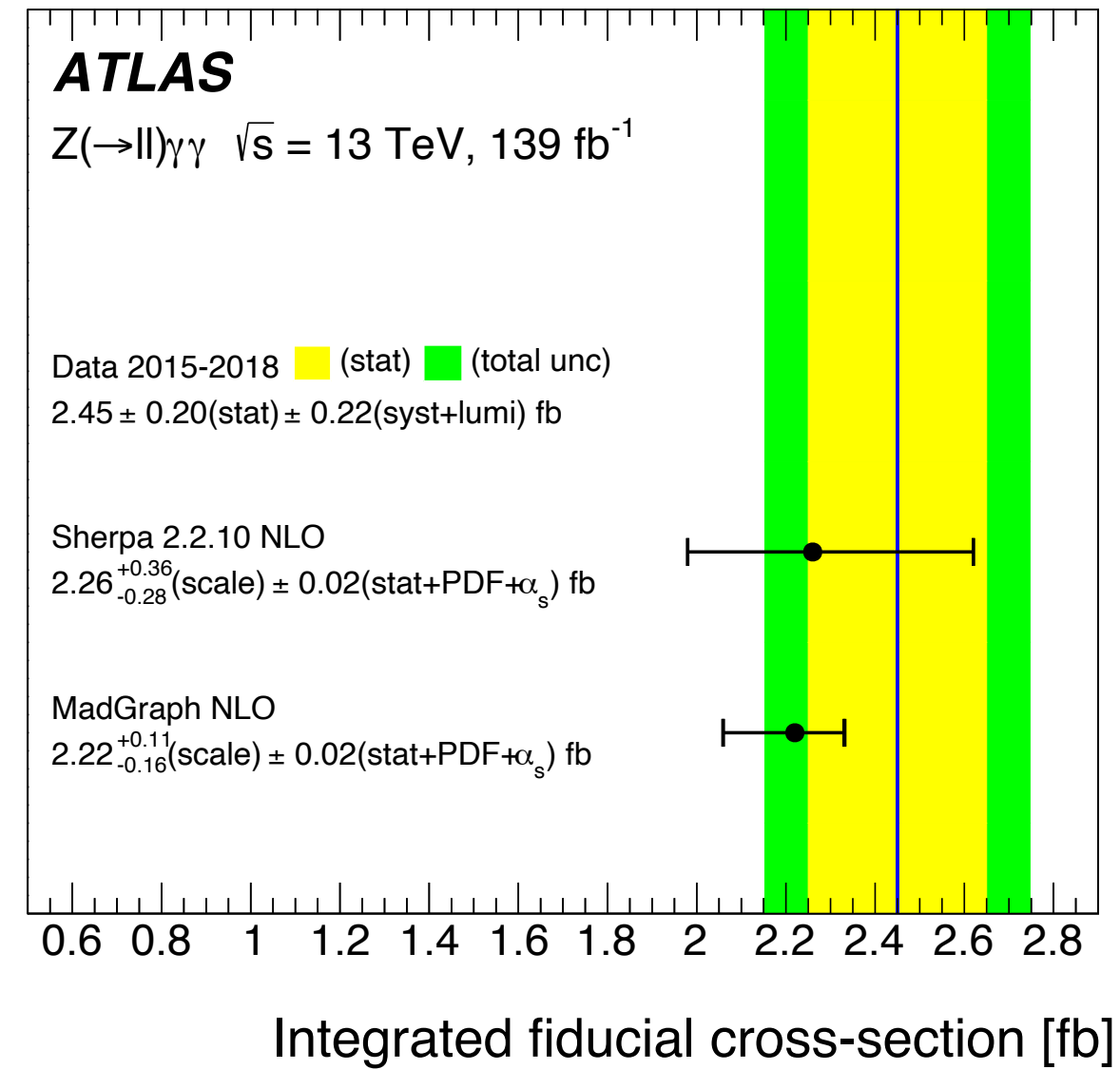
- Limits set on EFT Dim-8 operators.
- EFT contributions are suppressed above E_c . Parton level simulated events are scanned (before parton showering) and events with $m_{ll\gamma\gamma} > E_c$ are suppressed.
- Constraints are significantly stronger than any previous LHC results on neutral aQGCs.



Zγγ → 2lγγ

First observation at the LHC (rejecting FSR)

- A Z candidate and two photons with at least $\Delta R = 0.4$
- FSR contributions suppressed
- Dominant background is non-prompt photons. Background estimated from data. Largest source of systematic uncertainty
- Results consistent with SM predictions

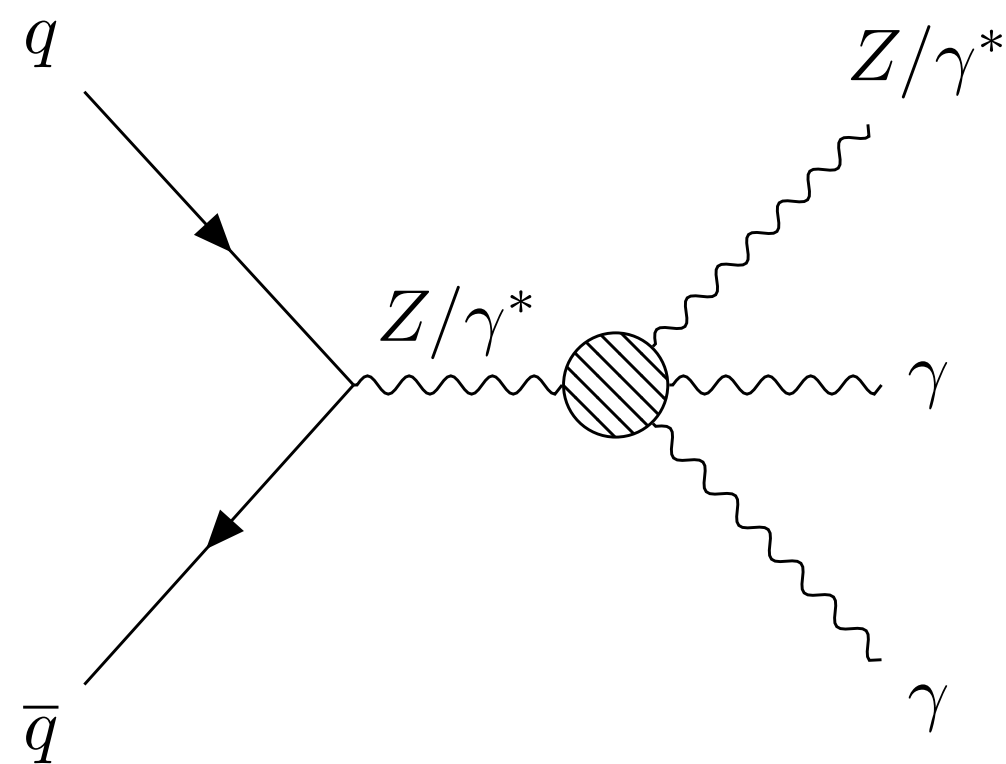


high p_T region

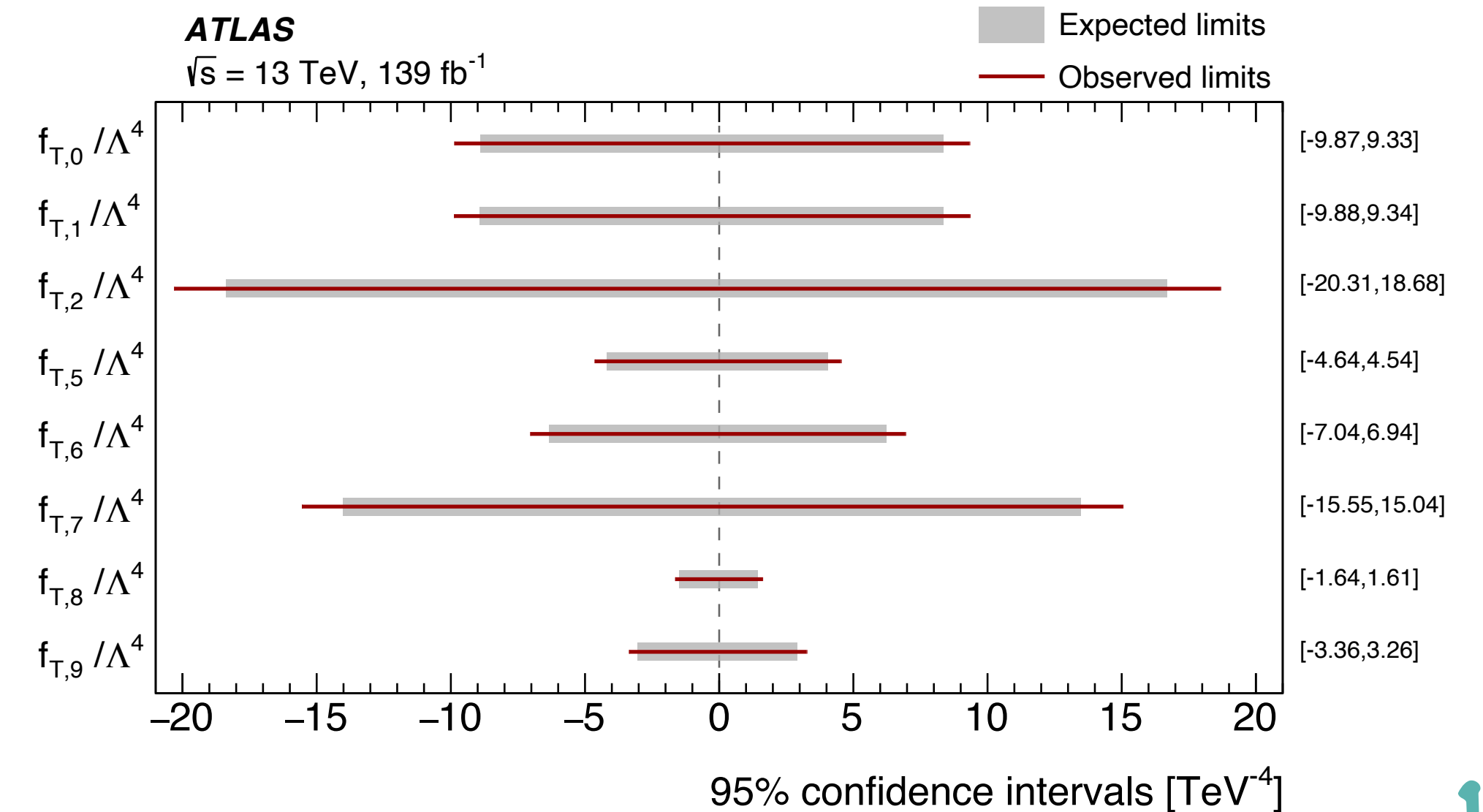
Limited accuracy in QCD modelling in the presence of jets

Not allowed in SM

ZZγγ, Zγγγ and γγγγ interactions possible via aQGCs

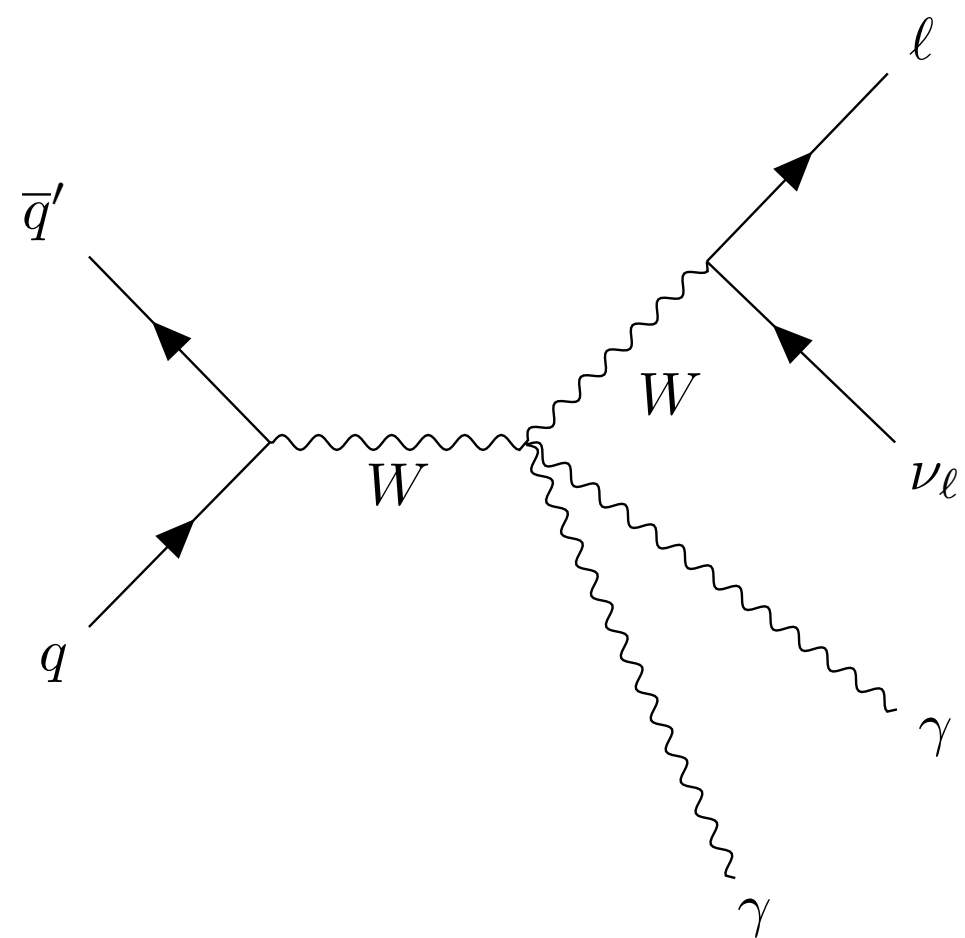


- Limits set on 8 Wilson coefficients of Dim-8 EFT operators.
- Constraints on 4 of the operators are two orders of magnitude more restrictive than the previous ATLAS result using 8 TeV
- Results are also obtained with clipping technique applied (backup)



$W\gamma\gamma \rightarrow l\nu\gamma\gamma$

First observation at the LHC



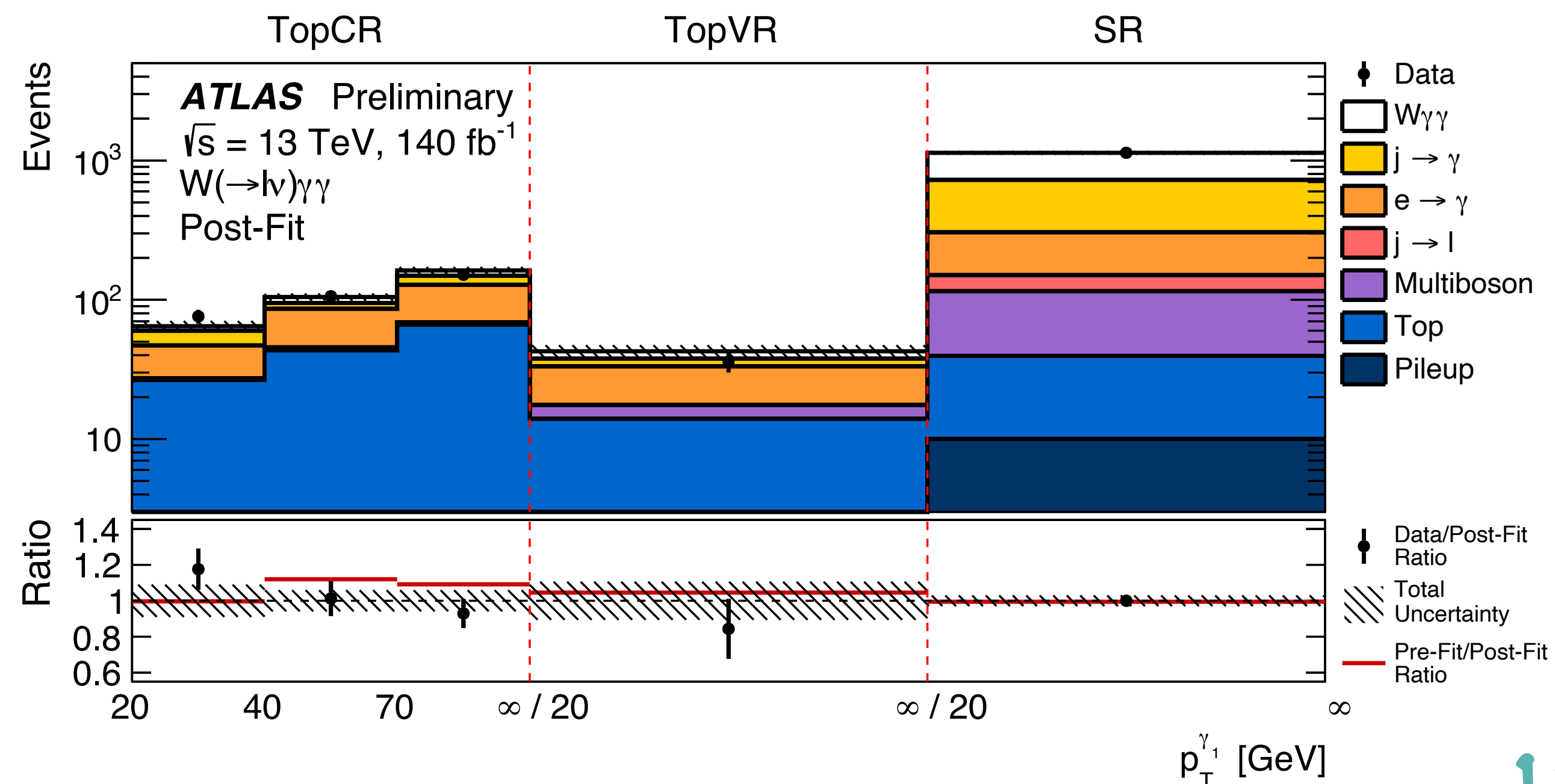
- A W boson candidate with $m_{T,W} > 40$ GeV and $E_T^{\text{miss}} > 25$ GeV
- $Z\gamma$ veto with $m_{l\gamma\gamma}, m_{l\gamma_1}, m_{l\gamma_2} \notin [82, 100]$ GeV
- b-jet veto to suppress top backgrounds
- Major background from non-prompt ($j \rightarrow \gamma$) and fake photons ($e \rightarrow \gamma$). Data-driven estimates
- Signal obtained from a binned maximum likelihood fit.
- Top background constrained in ≥ 1 b-jet CR simultaneously with SR. Validated in low E_T^{miss} region with ≥ 1 b-jet.

- Measured cross-section in agreement with SM predictions

$$\sigma_{fid} = 12.2^{+2.1}_{-2.0} \text{ fb}$$

Observed with 5.6σ (5.6σ expected)

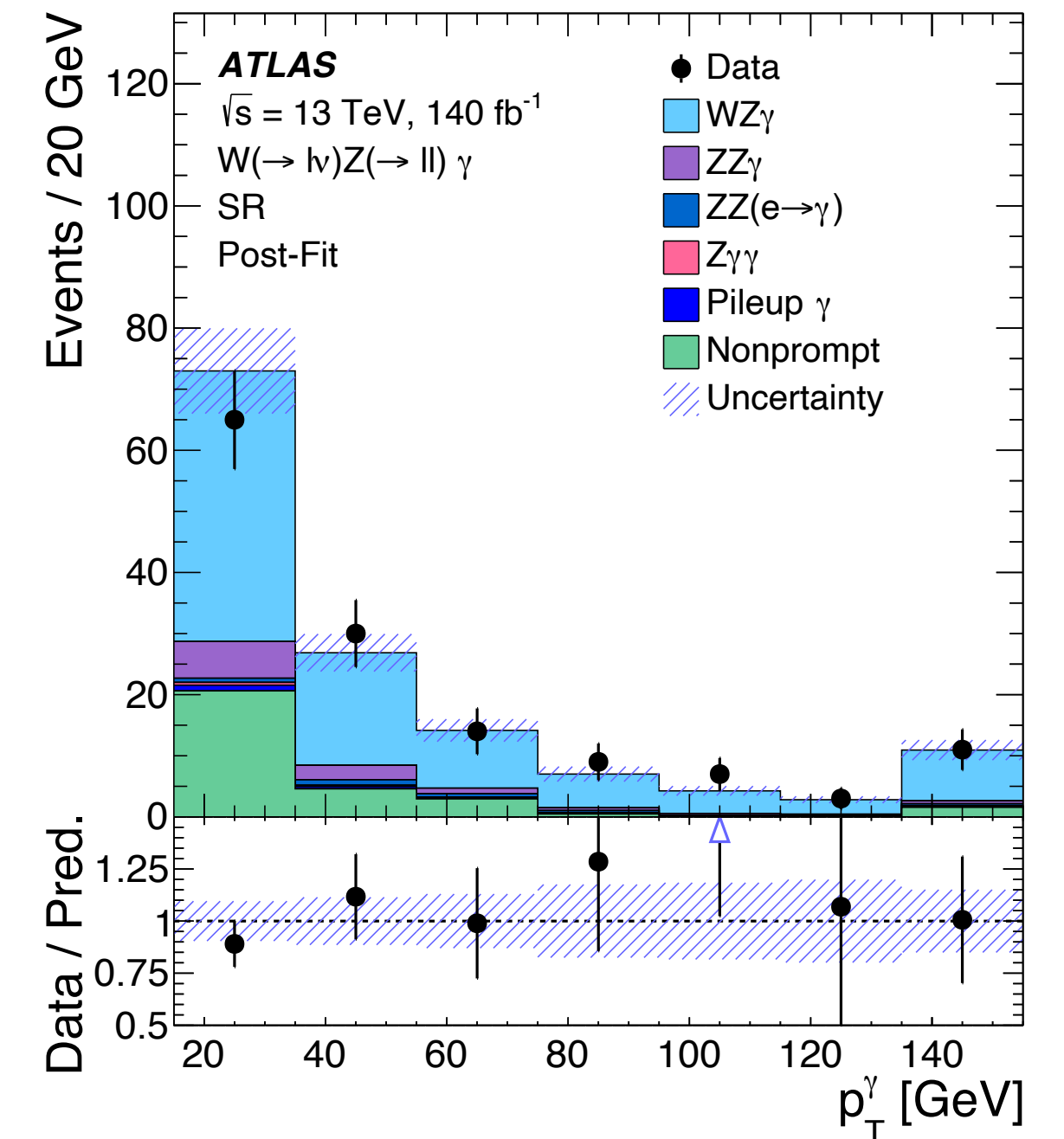
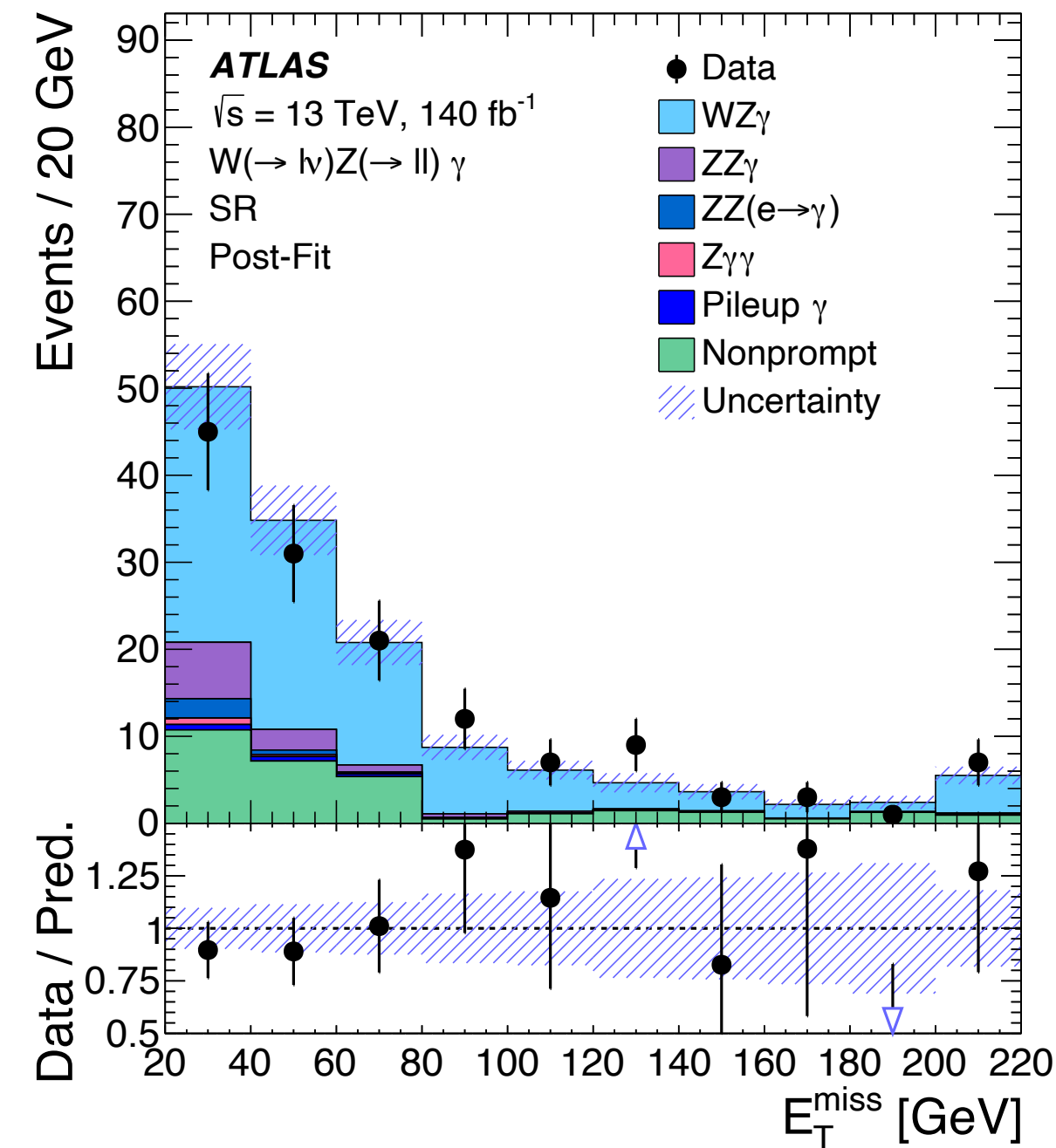
- Leading uncertainty source is the data-driven background estimates



WZ γ \rightarrow 3l $\nu\gamma$

First observation at the LHC

- Selections applied on p_T^l , p_T^γ , and E_T^{miss}
- Z candidate with m_{ll} closest to m_Z
- $m_{ll} > 81$ GeV suppresses FSR
- $|m_{e,\gamma} - m_Z| > 10$ GeV to reduce $e \rightarrow \gamma$
- Dominant background is non-prompt leptons and photons
- Signal extracted from a maximum likelihood fit in SR and ZZ γ CR and ZZ($e \rightarrow \gamma$) CR
- ZZ γ and ZZ normalizations obtained from the CRs
- Leading uncertainty is limited data statistics
- Systematic uncertainty dominated by statistical uncertainty in non-prompt background estimation



- Measured cross-section agrees with SM predictions within 1.5σ

$$\sigma_{fid} = 2.01 \pm 0.34 \text{ fb}$$

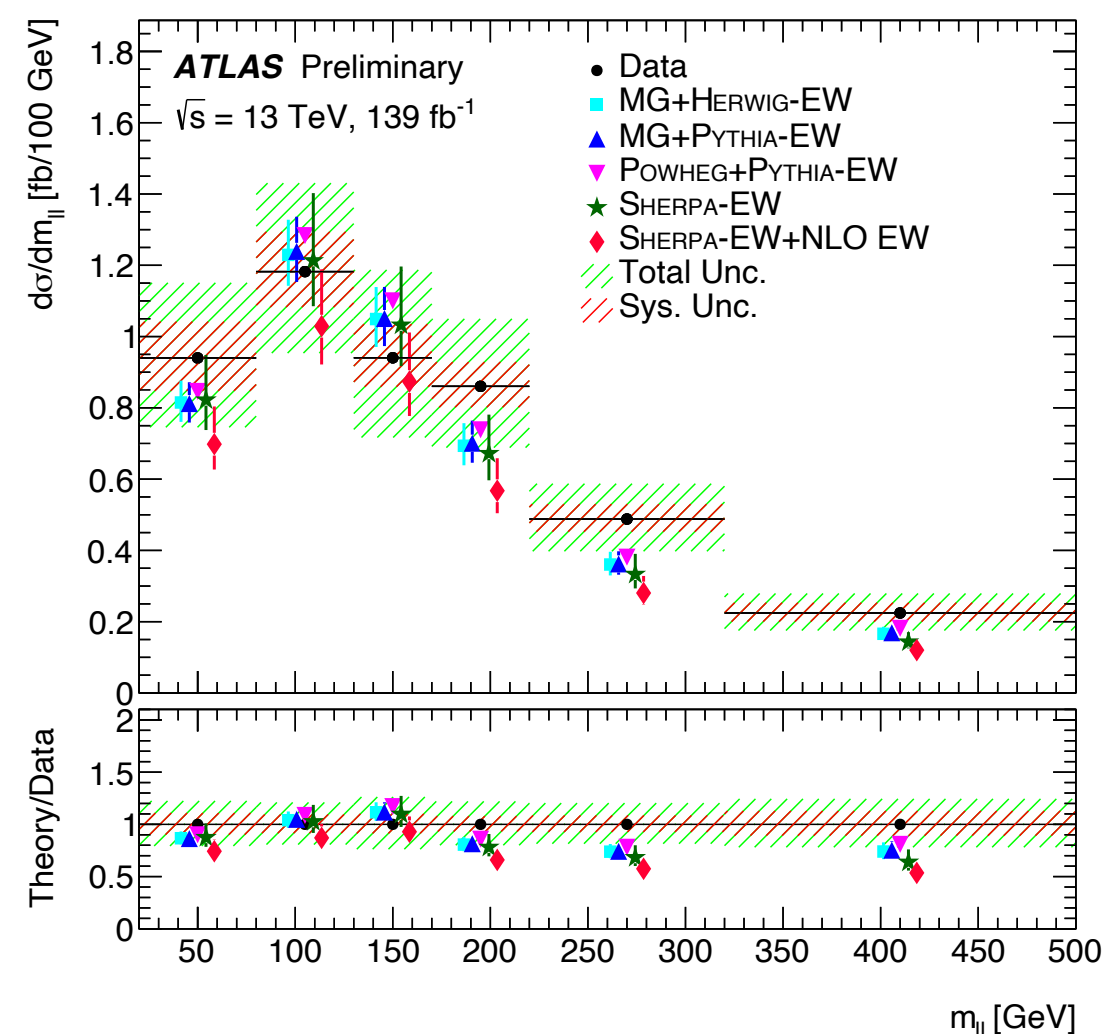
Observed with 6.3σ (5.0σ expected)

Summary

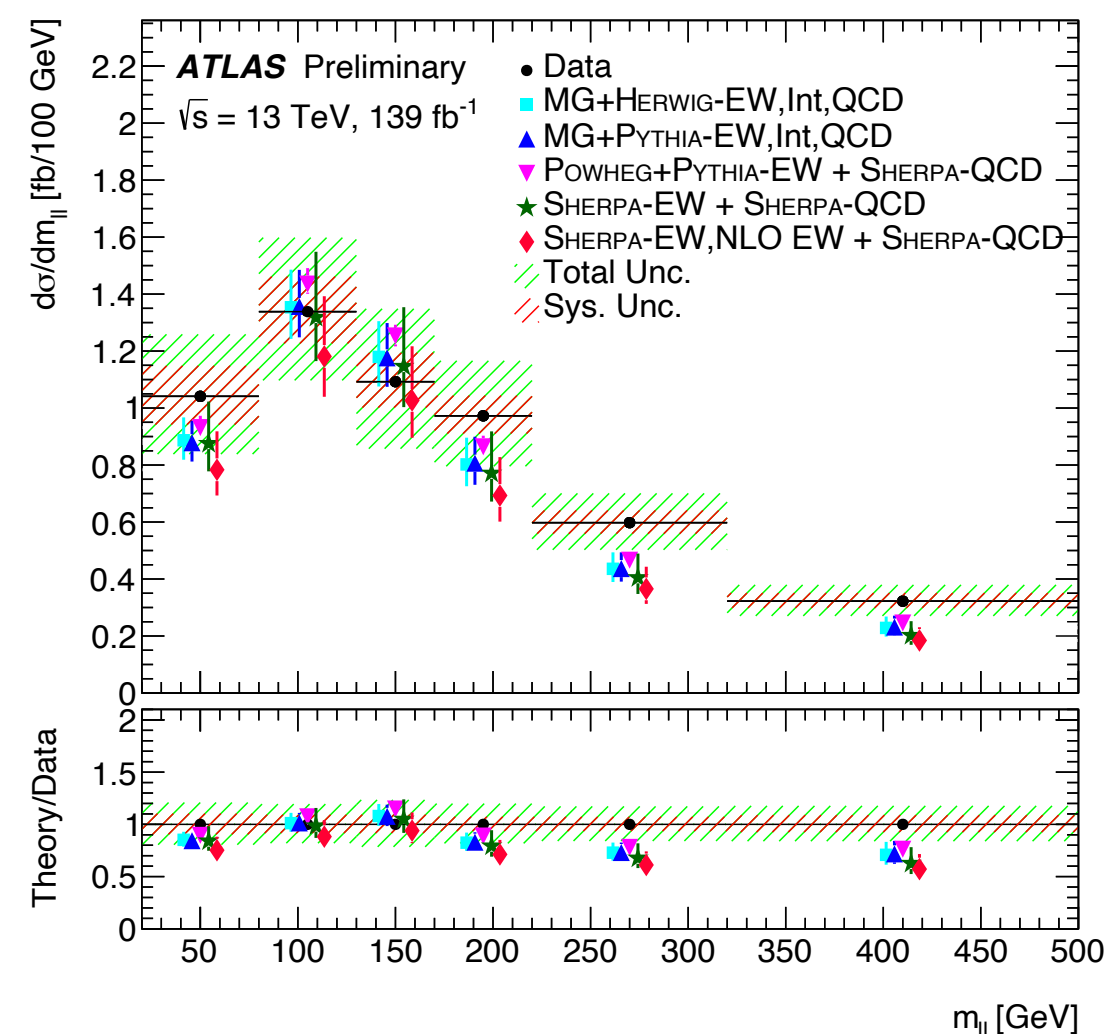
- Multiboson interactions with tree level sensitivity to quartic gauge couplings serve as a powerful tool to stringently test SM predictions
- Probes extreme phase spaces which became experimentally accessible for the first time in LHC Run 2
- Most of these processes have been observed in Run 2 with some already in the measurement phase
- Many exciting first observations in ATLAS!
- All results are compatible with SM predictions so far
- Results are interpreted in the context of EFT and limits are set on Dim-6 and Dim-8 operators
- LHC will continue to test SM with better sensitivities to new physics in Run 3 and beyond!

Backup

$W^\pm W^\pm (\rightarrow 2l2\nu) + \text{jets}$



Electroweak production



Inclusive production

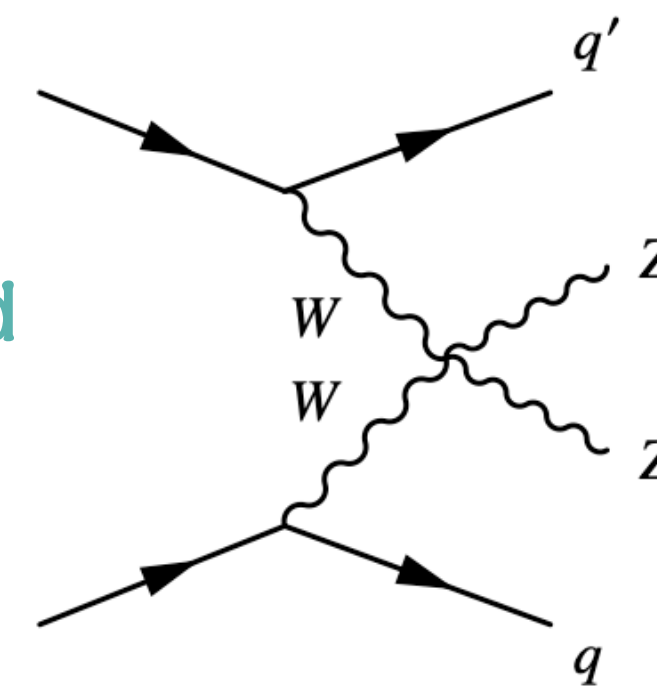
Variable	EW $W^\pm W^\pm jj$		Inclusive $W^\pm W^\pm jj$	
	χ^2/N_{dof}	p -value	χ^2/N_{dof}	p -value
$m_{\ell\ell}$	4.4/6	0.623	7.0/6	0.322
m_T	12.9/6	0.045	15.9/6	0.014
m_{jj}	7.2/6	0.300	7.8/6	0.250
$N_{\text{gap jets}}$	2.3/2	0.316	2.3/2	0.316
ξ_{j_3}	4.3/5	0.511	5.2/5	0.396

- Differential cross-section measured for electroweak and inclusive production
- Likelihood based unfolding for correction to particle level
- Leading uncertainty from data statistics

Source	Impact [%]
Experimental	
Electron calibration	0.4
Muon calibration	0.5
Jet energy scale and resolution	1.8
E_T^{miss} scale and resolution	0.2
b -tagging inefficiency	0.7
Background, misid. leptons	3.1
Background, charge misrec.	0.8
Pileup modelling	0.2
Luminosity	1.9
Modelling	
EW $W^\pm W^\pm jj$, shower, scale, PDF & α_s	0.8
EW $W^\pm W^\pm jj$, QCD corrections	3.5
EW $W^\pm W^\pm jj$, EW corrections	0.8
Int $W^\pm W^\pm jj$, shower, scale, PDF & α_s	0.1
QCD $W^\pm W^\pm jj$, shower, scale, PDF & α_s	2.3
QCD $W^\pm W^\pm jj$, QCD corrections	0.9
Background, WZ scale, PDF & α_s	0.2
Background, WZ reweighting	1.7
Background, other	1.0
Model statistical	1.8
Experimental and modelling	6.7
Data statistical	7.4
Total	10.0

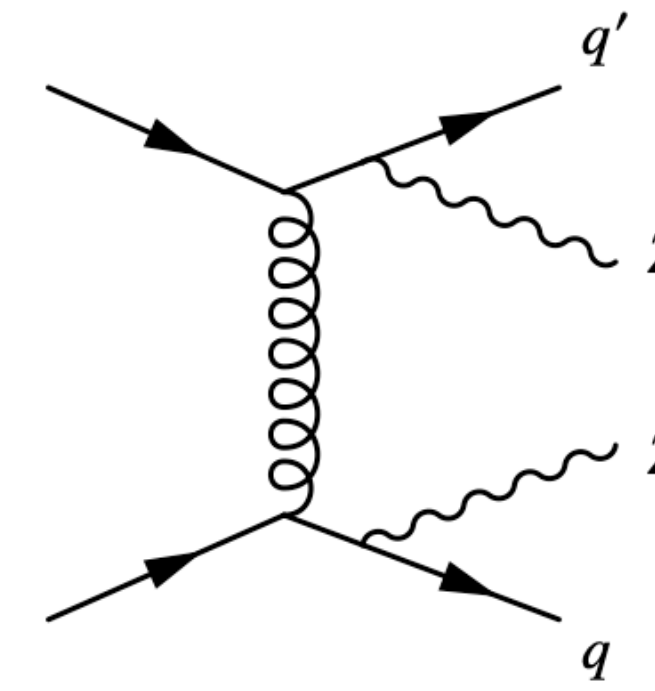
ZZ($\rightarrow 4l$) + jets

sensitive to WWZ and WWZZ interactions



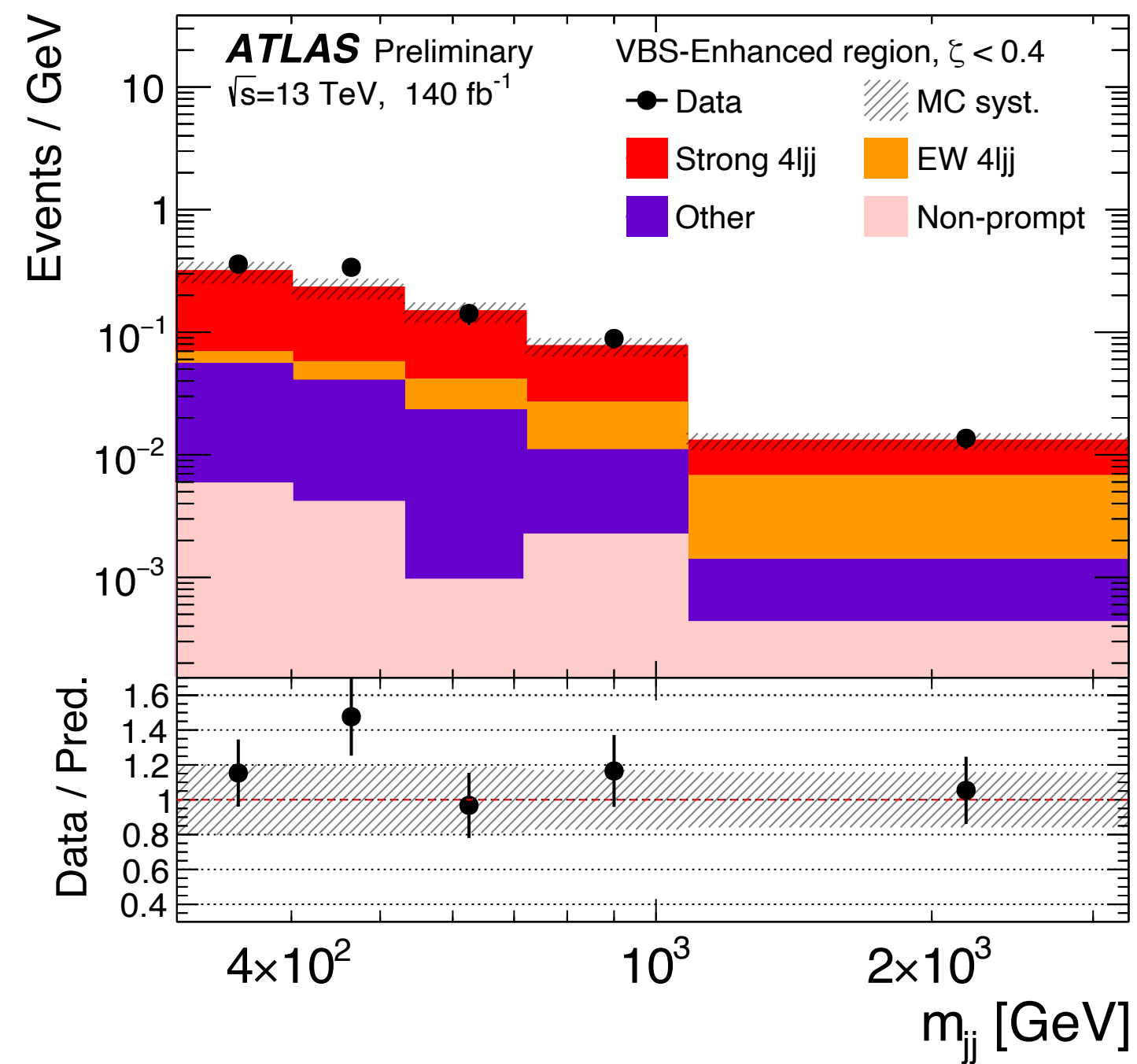
electroweak

sensitive to perturbative QCD calculations

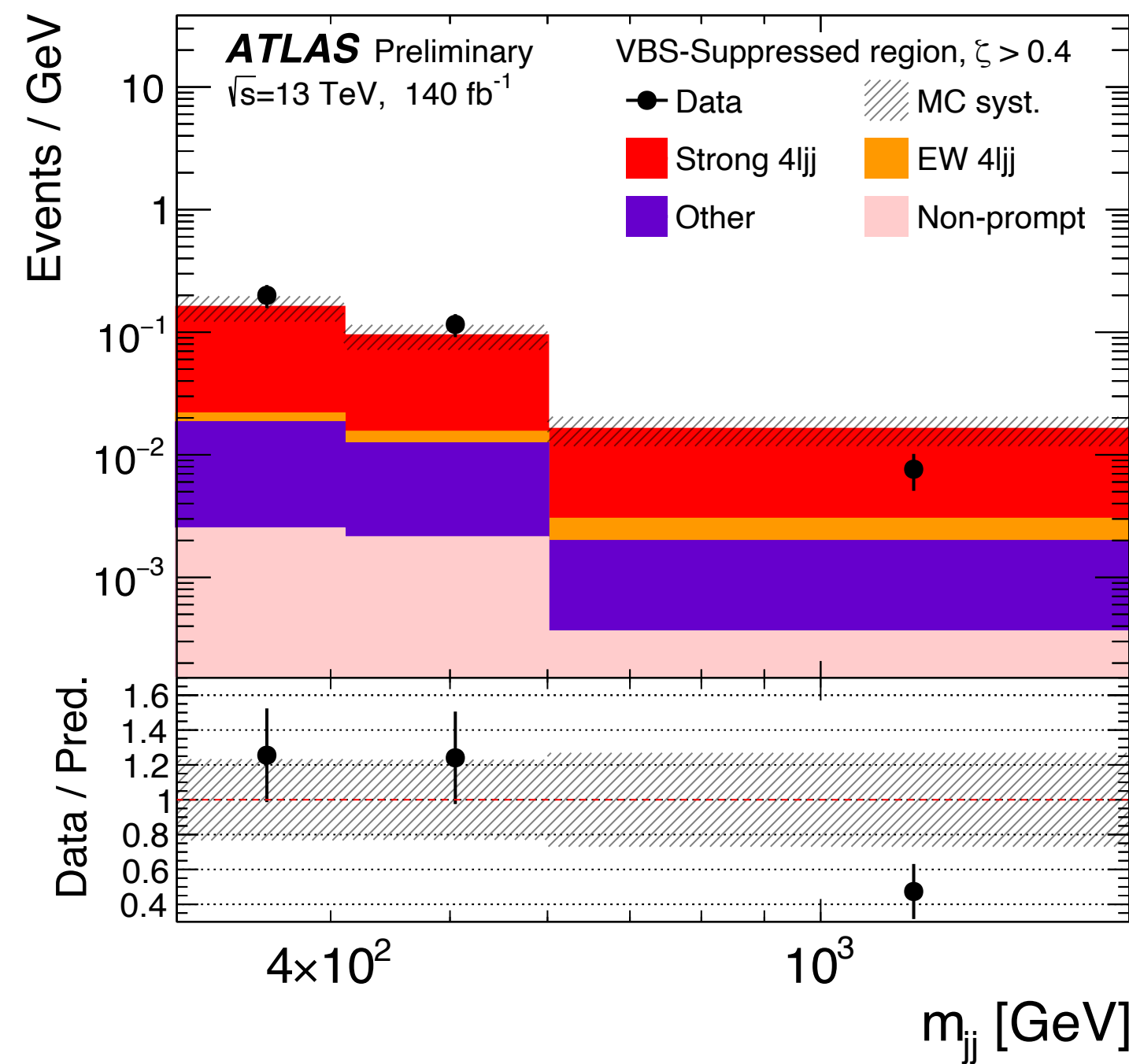


strong

VBS enhanced



VBS suppressed

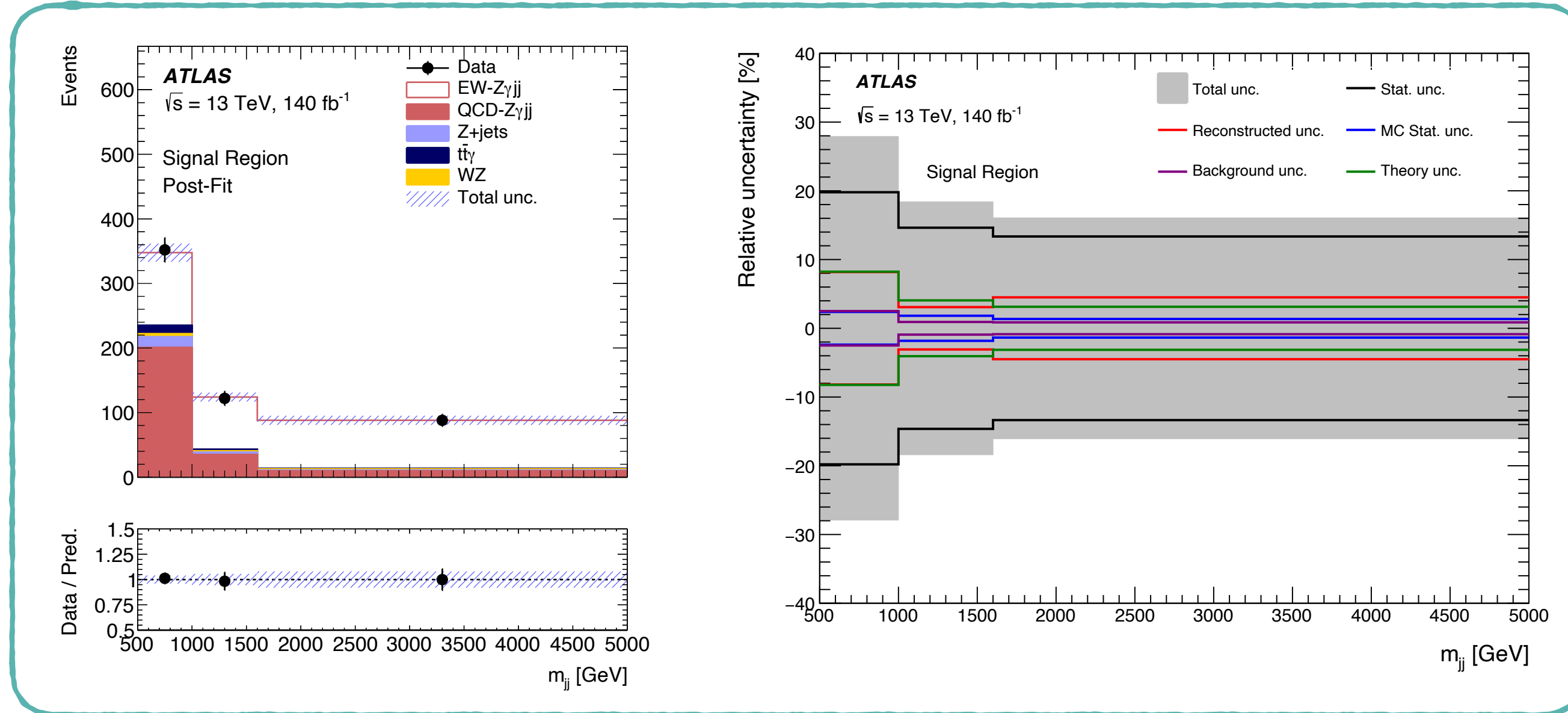


$$\zeta = \frac{y_{4l} - 0.5(y_{j_1} + y_{j_2})}{\Delta y_{jj}}$$

VBS enhanced SR with $\zeta < 0.4$

VBS suppressed SR with $\zeta > 0.4$

Z γ (\rightarrow 2 γ) + jets

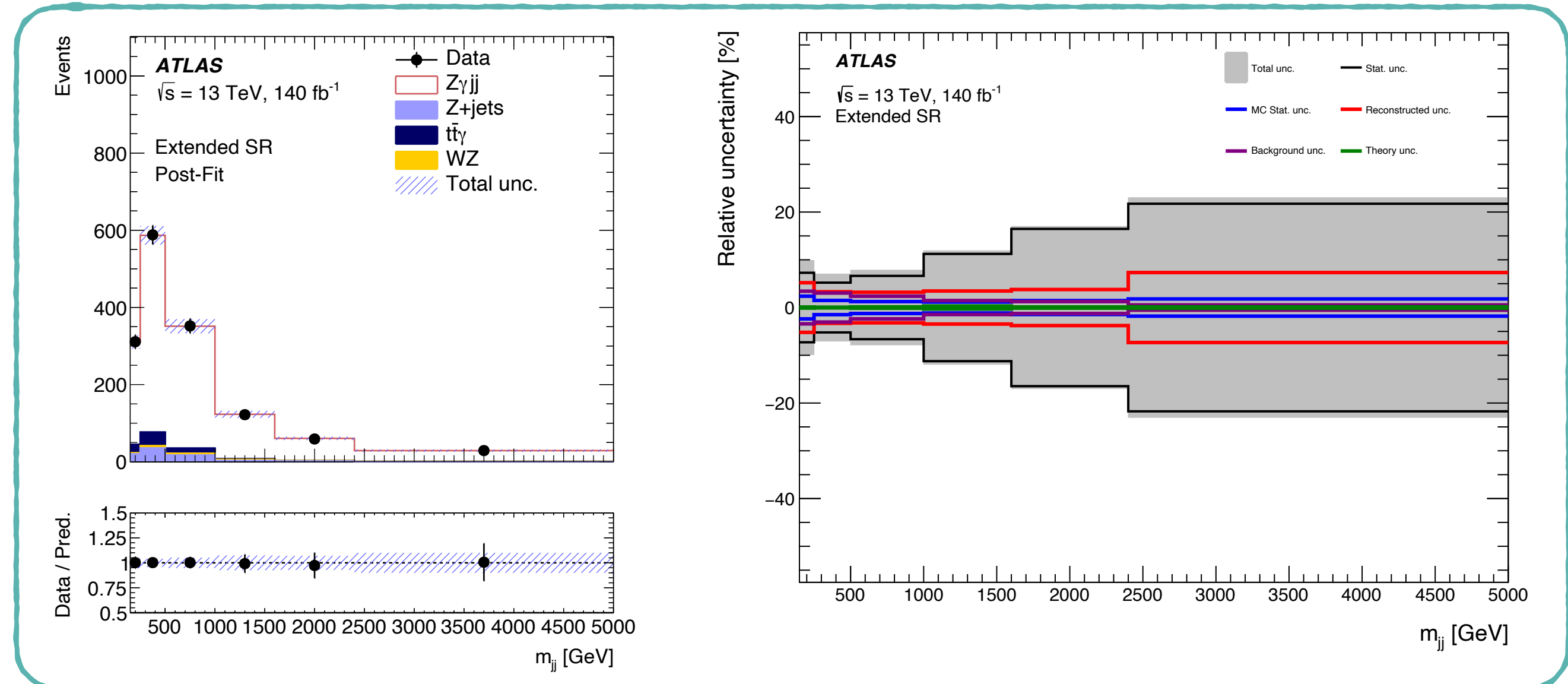


Z γ -EWK SR
 $m_{jj} > 500$ GeV
 $\zeta < 0.4$

Inclusive Z γ SR
 $m_{jj} > 150$ GeV
 $\zeta < 0.4$

Inclusive Z γ SR

Z γ -EWK SR



$Z\gamma(\rightarrow 2\nu\gamma) + \text{jets}$

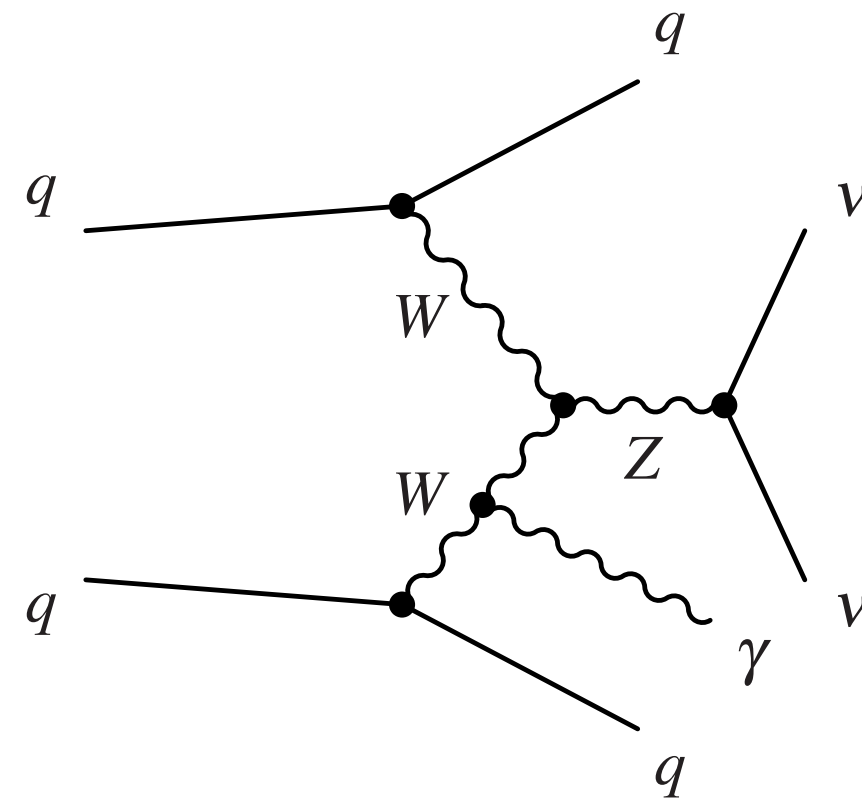
Eur. Phys. J. C 82 (2022) 105

$$15 < E_T^\gamma < 110 \text{ GeV}$$

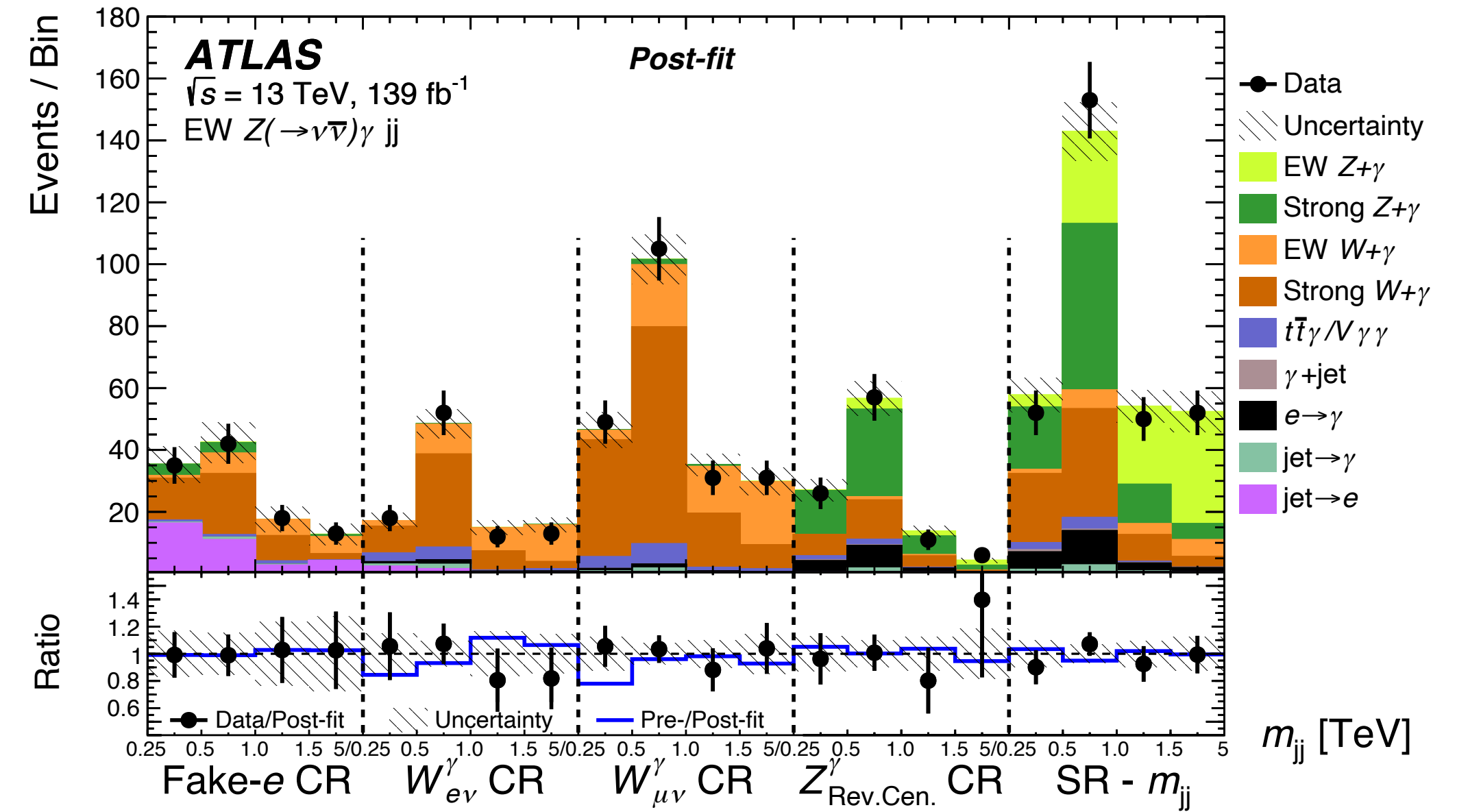
Not sensitive to aQGC search

Observed with 5.2σ

started as a search for BSM Higgs decays

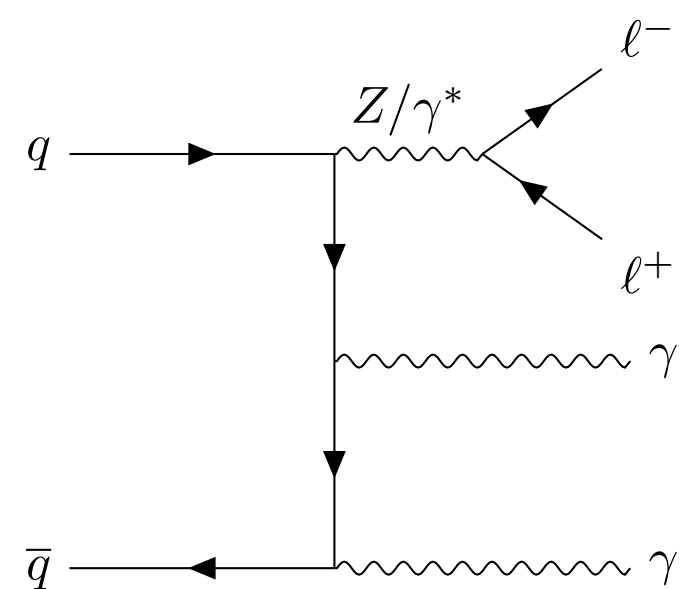


- Dominant backgrounds from $W\gamma$ and QCD induced $Z\gamma$
- Signal obtained from a binned maximum likelihood fit of CR and SR

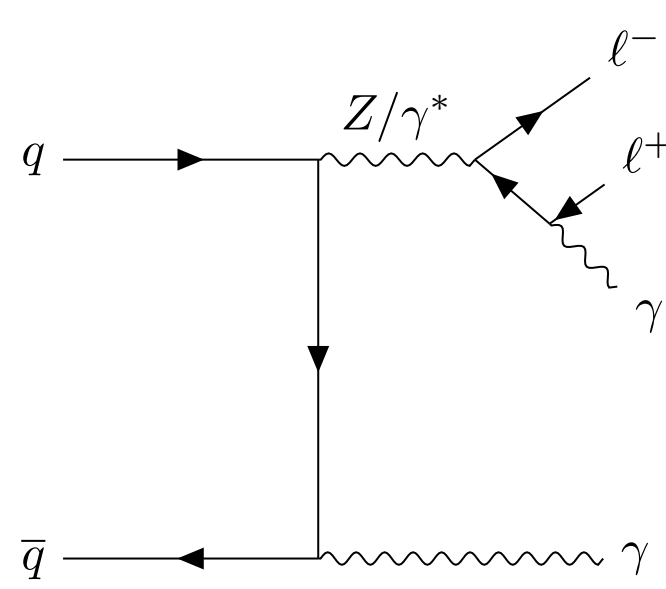


$\mu_{Z\gamma_{EW}}$	$\beta_{Z\gamma_{strong}}$	$\beta_{W\gamma}$
1.03 ± 0.25	1.02 ± 0.41	1.01 ± 0.20

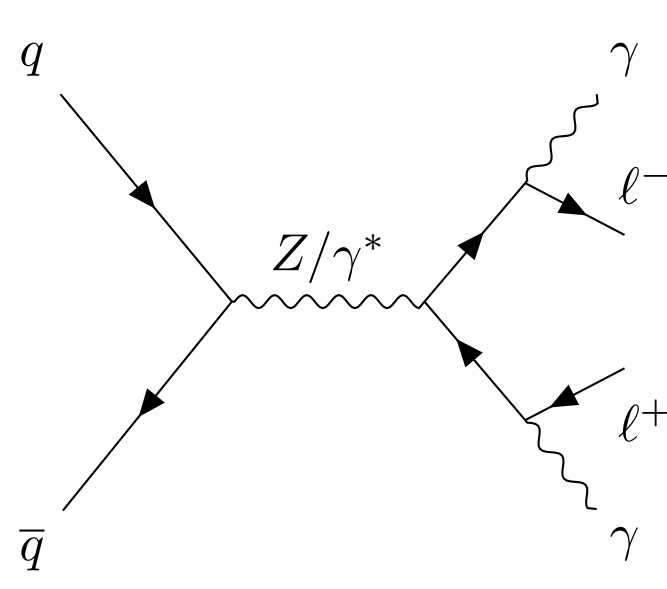
Z $\gamma\gamma$ \rightarrow 2l $\gamma\gamma$



ISR

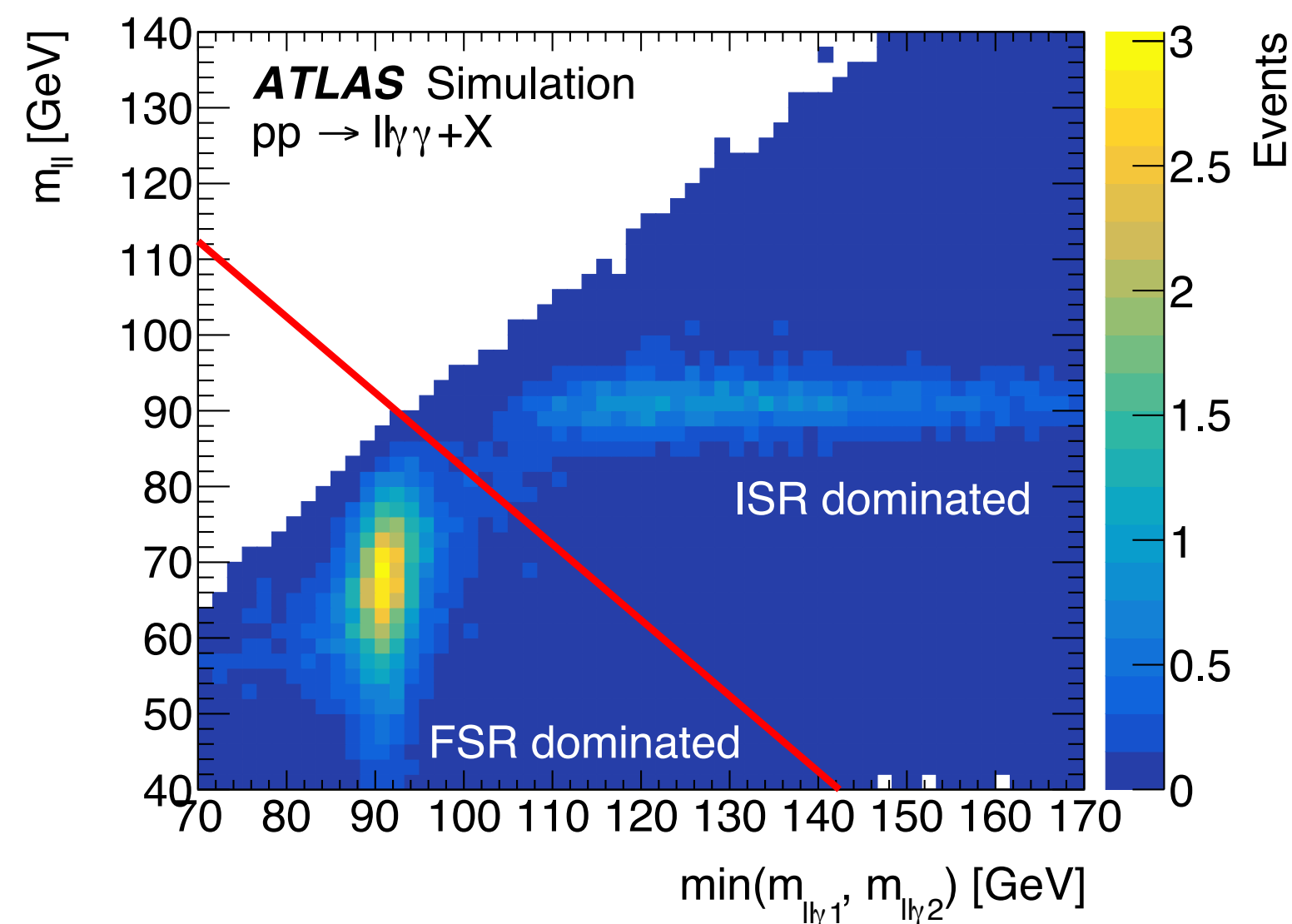


FSR

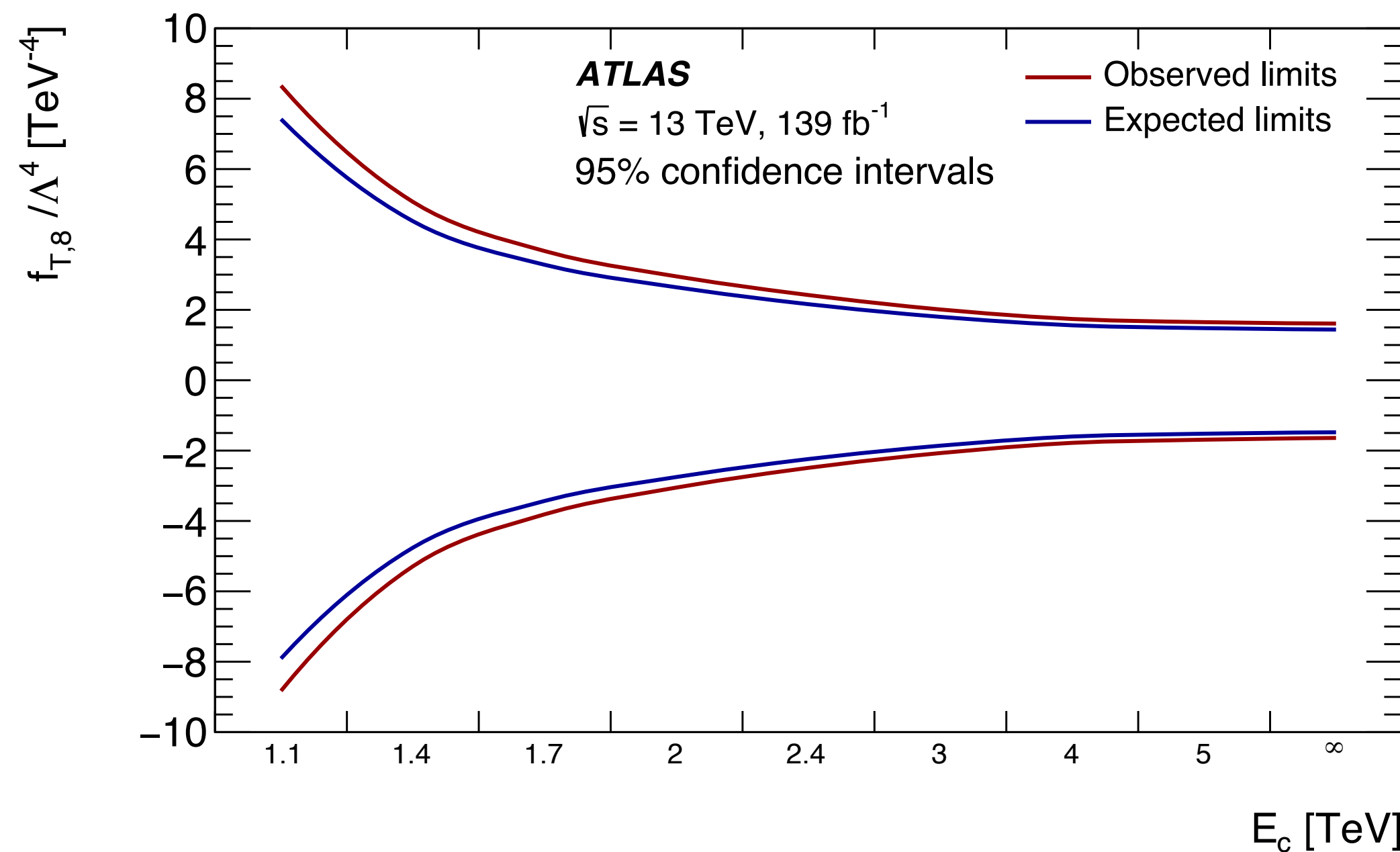


FSR

Source	Relative uncertainty [%]	
	$e^+e^-\gamma\gamma$	$\mu^+\mu^-\gamma\gamma$
Photon identification efficiency	2.5	2.6
Photon isolation efficiency	2.0	2.0
Electron-photon energy resolution	0.2	0.1
Electron-photon energy scale	0.8	0.6
Electron identification efficiency	2.0	-
Electron reconstruction efficiency	0.3	-
Muon isolation efficiency	-	0.4
Muon reconstruction efficiency	-	0.4
Muon trigger efficiency	-	0.3
Muon momentum scale	-	0.2
Pile-up reweighting	2.8	2.9
Monte Carlo signal statistics	1.1	1.0
Signal modelling	1.1	1.1
Integrated luminosity	1.7	1.7
$j \rightarrow \gamma$ backgrounds	7.5	7.6
Other backgrounds	1.7	1.9
Total systematic uncertainty	8.6	7.5
Data statistical uncertainty	11.5	10.9
Total uncertainty	14.5	13.3

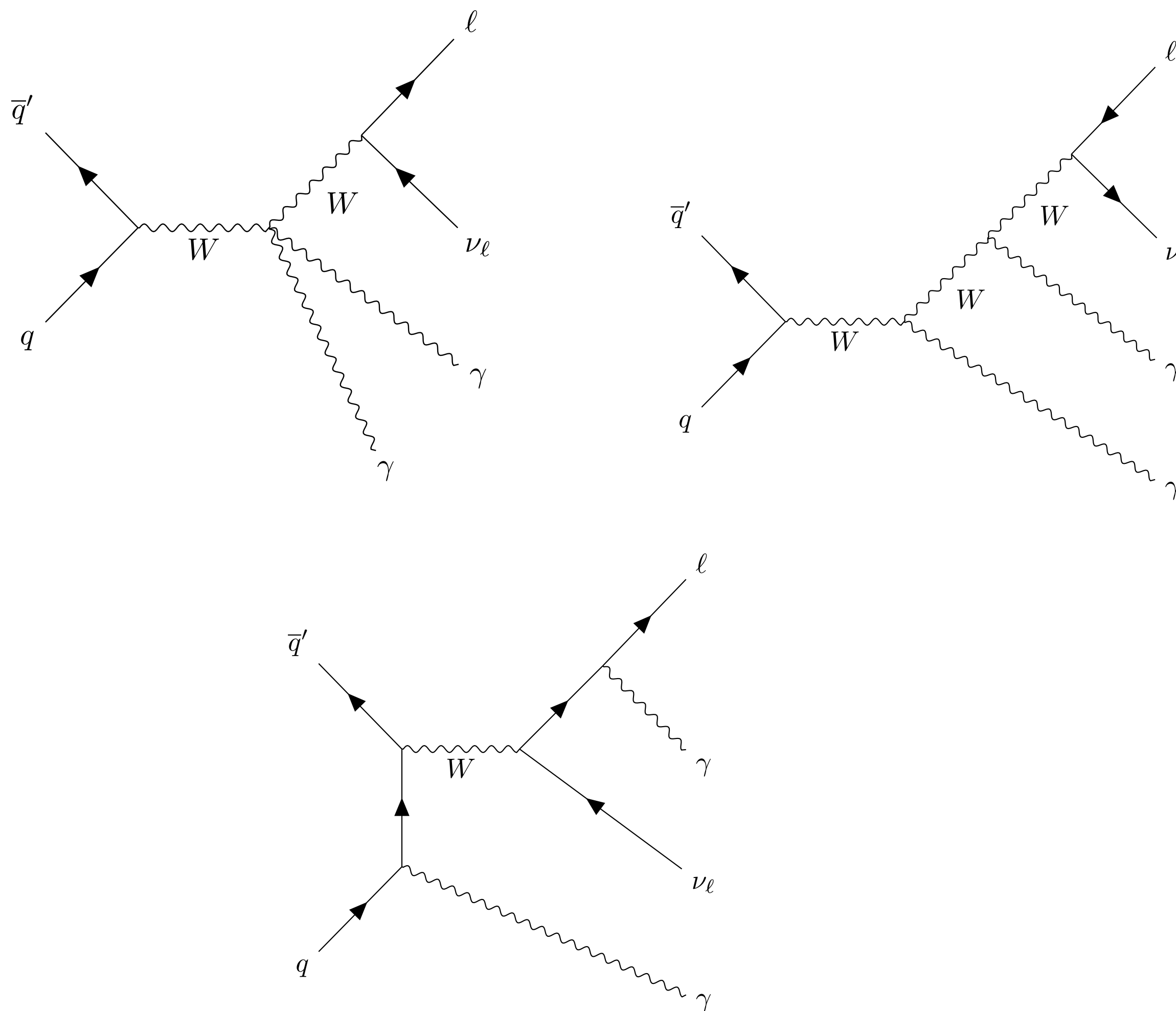


$$m_{ll} + \min(m_{ll\gamma 1}, m_{ll\gamma 2}) > 2m_Z$$



$W\gamma\gamma \rightarrow \ell\nu\gamma\gamma$

First observation at the LHC

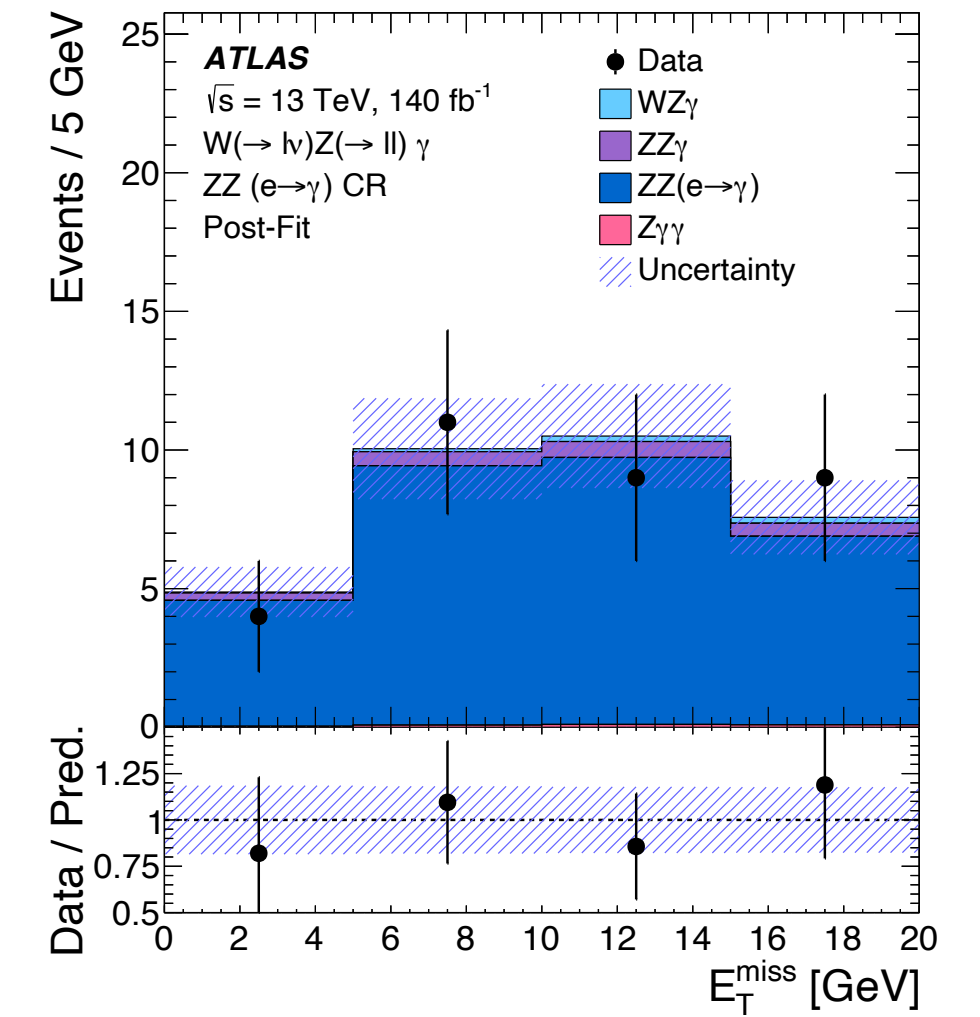
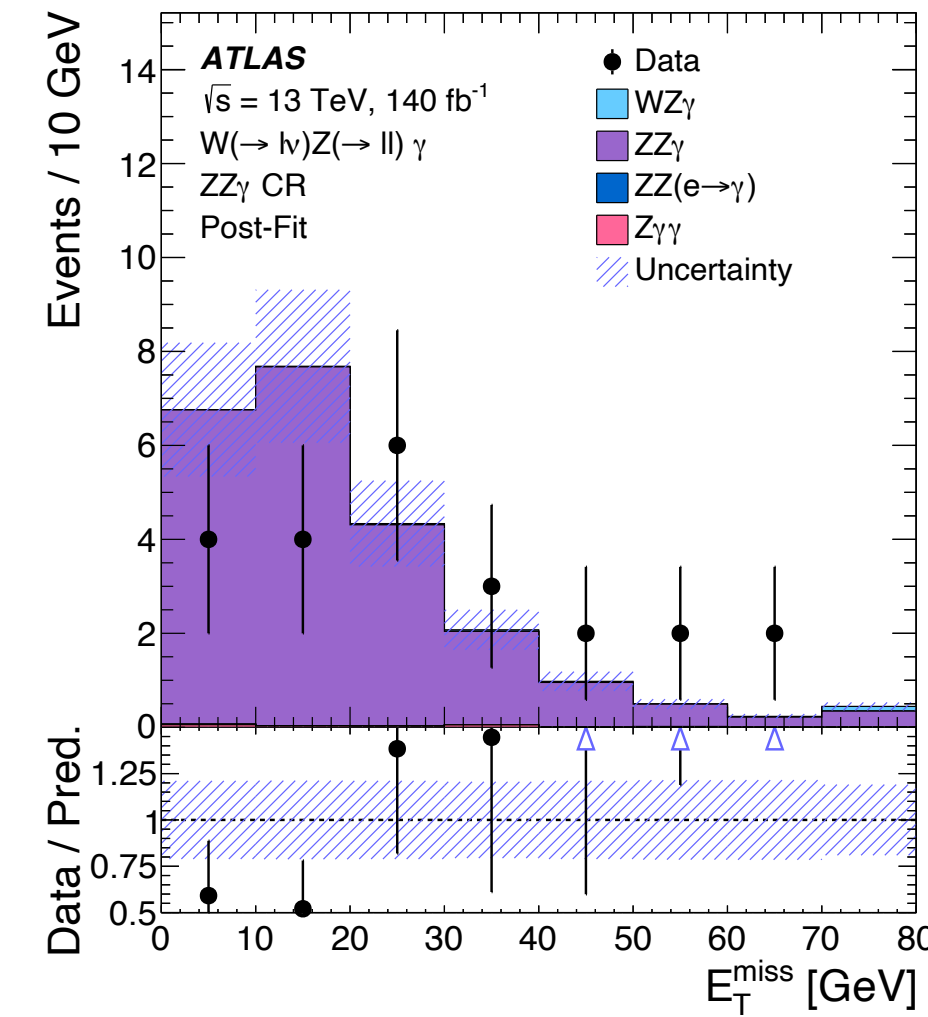
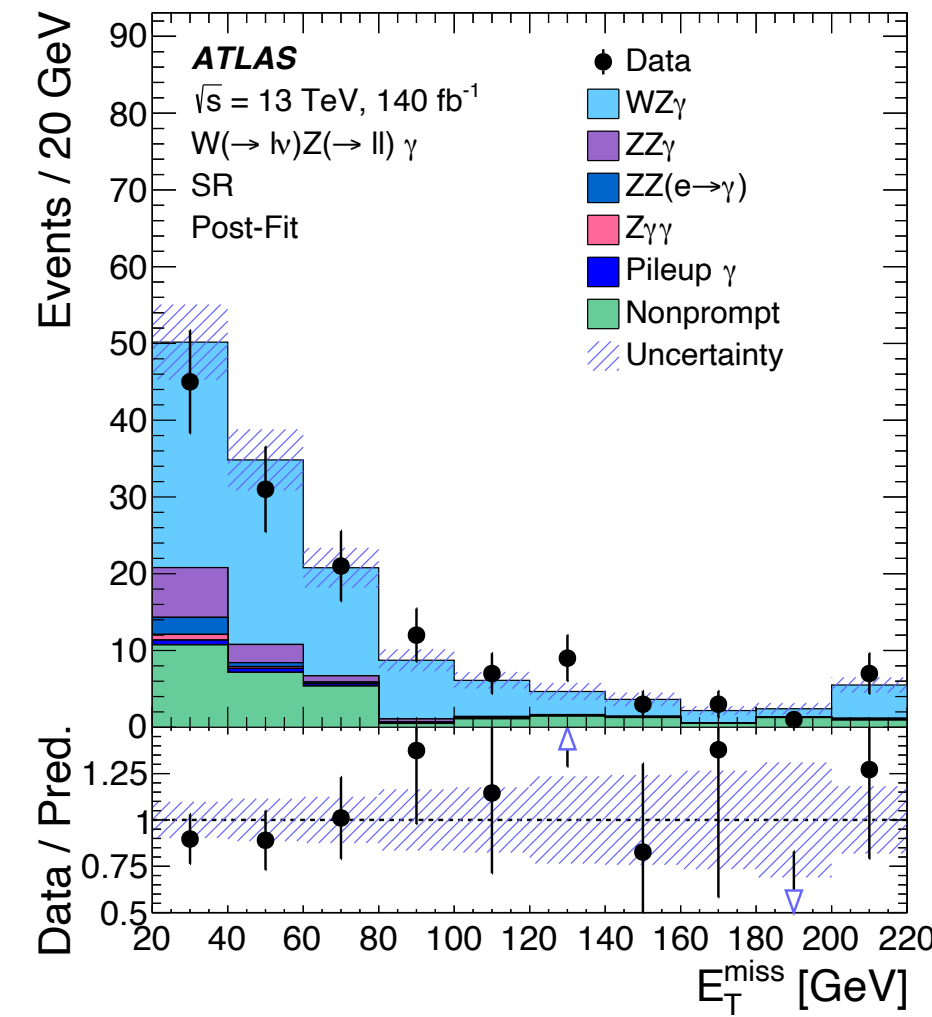
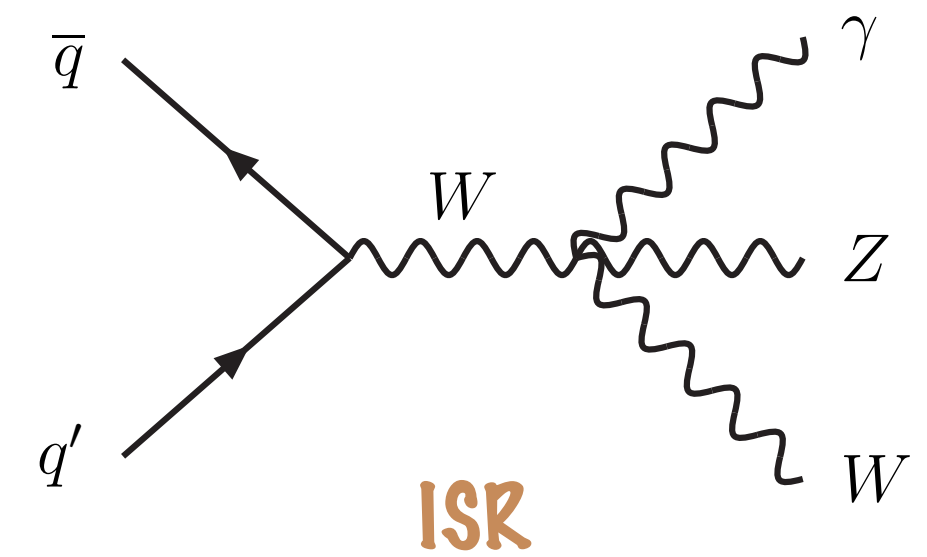
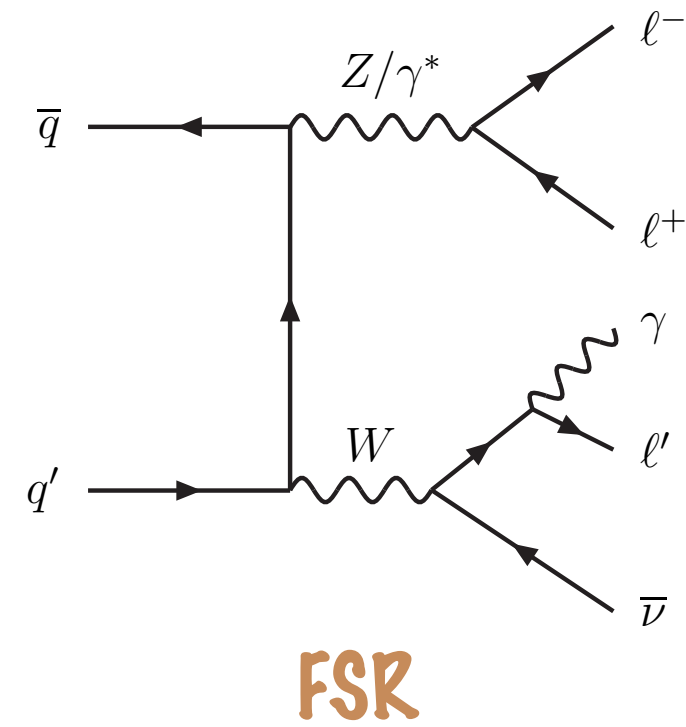
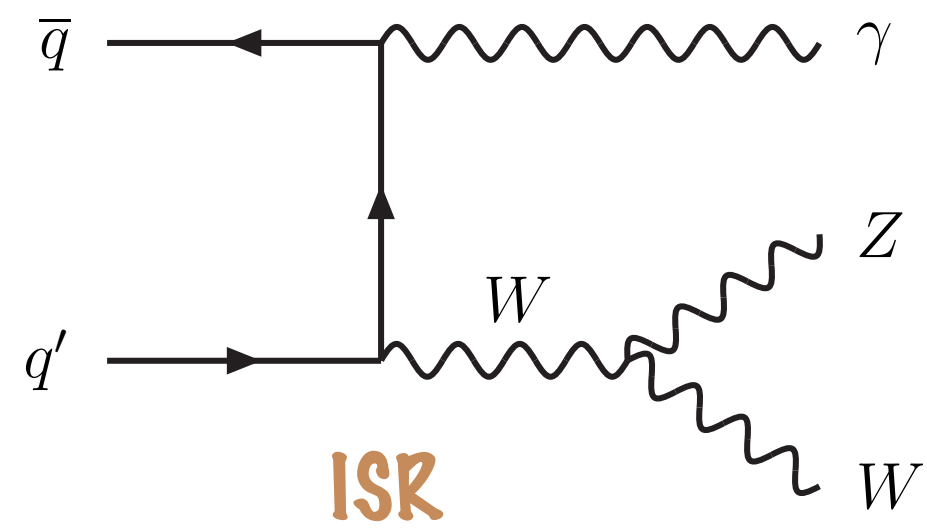


Source	SR	TopCR
$W\gamma\gamma$	410 ± 60	28 ± 5
Non-prompt $j \rightarrow \gamma$	420 ± 50	42 ± 20
Misidentified $e \rightarrow \gamma$	155 ± 11	120 ± 9
Multiboson ($WH(\gamma\gamma)$, $WW\gamma$, $Z\gamma\gamma$)	76 ± 13	5.2 ± 1.7
Non-prompt $j \rightarrow \ell$	35 ± 10	–
Top ($tt\gamma$, $tW\gamma$, $tq\gamma$)	30 ± 7	136 ± 32
Pileup	10 ± 5	–
Total	$1\,136 \pm 34$	332 ± 18
Data	1 136	333

Source of uncertainty	Impact [%]
Data-driven background estimates	13
Photon efficiency	4.5
Signal MC theoretical modeling	3.5
Background MC theoretical modeling	3.0
Monte Carlo statistics	2.8
Jet efficiency and calibration	2.4
Top normalization	2.4
Pileup reweighting	1.6
E_T^{miss} calibration	1.4
Muon efficiency and calibration	1.4
Luminosity	1.0
Electron and photon calibration	0.7
Flavor tagging efficiency	0.6
Systematic	15
Statistical	8.3
Total	17

$WZ\gamma \rightarrow 3l\nu\gamma$

First observation at the LHC



Process	SR	$ZZ\gamma$ CR	$ZZ(e\rightarrow\gamma)$ CR
$WZ\gamma$	92 ± 15	0.21 ± 0.07	0.56 ± 0.14
$ZZ\gamma$	10.7 ± 2.3	23 ± 5	1.8 ± 0.4
$ZZ(e\rightarrow\gamma)$	3.0 ± 0.6	0.028 ± 0.020	30 ± 6
$Z\gamma\gamma$	1.05 ± 0.32	0.15 ± 0.06	0.29 ± 0.10
Nonprompt background	30 ± 6	-	-
Pileup γ	1.9 ± 0.7	-	-
Total yield	139 ± 12	23 ± 5	33 ± 6
Data	139	23	33